ESAIM: M2AN 55 (2021) S225–S250
https://doi.org/10.1051/m2an/2020028

ESAIM: Mathematical Modelling and Numerical Analysis
www.esaim-m2an.org

A CONVERGENT CONVEX SPLITTING SCHEME FOR A NONLOCAL CAHN–HILLIARD–OONO TYPE EQUATION WITH A TRANSPORT TERM

Laurence Cherfils[1], Hussein Fakih[2,3,*], Maurizio Grasselli[4] and Alain Miranville[5,6]

Abstract. We devise a first-order in time convex splitting scheme for a nonlocal Cahn–Hilliard–Oono type equation with a transport term and subject to homogeneous Neumann boundary conditions. However, we prove the stability of our scheme when the time step is sufficiently small, according to the velocity field and the interaction kernel. Furthermore, we prove the consistency of this scheme and the convergence to the exact solution. Finally, we give some numerical simulations which confirm our theoretical results and demonstrate the performance of our scheme not only for phase separation, but also for crystal nucleation, for several choices of the interaction kernel.

Mathematics Subject Classification. 34K28, 35R09, 65M12, 65M60, 82C26.

Received June 29, 2018. Accepted April 17, 2020.

1. Introduction

1.1. Cahn–Hilliard equation

The authors proposed in [8] the following Ginzburg–Landau type free energy:

$$\mathcal{E}_{\mathrm{CH}}(\varphi) = \int_\Omega \left(\frac{\varepsilon^2}{2} |\nabla \varphi|^2 + F(\varphi) \right) \mathrm{d}x, \tag{1.1}$$

in order to describe the phase separation of a binary mixture, and, more precisely, the so-called spinodal decomposition. Here, $\Omega \subset \mathbb{R}^N$, $N \leqslant 3$, is a bounded domain occupied by the mixture components A and B,

Keywords and phrases. Cahn–Hilliard–Oono equation, transport term, nonlocal term, convex splitting scheme, stability and convergence, numerical simulations.

[1] Université de La Rochelle, Laboratoire des Sciences de l'Ingénieur pour l'Environnement, UMR CNRS 7356, Avenue Michel Crépeau, La Rochelle Cedex F-17042, France.

[2] Lebanese International University, Department of Mathematics and Physics, Beqaa Campus, Lebanon.

[3] Lebanese University, Department of Mathematics, Beirut, Lebanon.

[4] Politecnico di Milano – Dipartimento di Matematica, Milano I-20133, Italy.

[5] Université de Poitiers, Laboratoire de Mathématiques et Applications, UMR CNRS 7348 – SP2MI, Boulevard Marie et Pierre Curie – Téléport 2, Chasseneuil Futuroscope Cedex F-86962, France.

[6] Xiamen University, School of Mathematical Sciences, Fujian Provincial Key Laboratory of Mathematical Modeling and High Performance Scientific Computing, Xiamen, Fujian, P.R. China.

*Corresponding author: hussein.fakih@liu.edu.lb

with respective mass fractions φ_A and φ_B, and the order parameter is defined by $\varphi = \frac{\varphi_A - \varphi_B}{\varphi_A + \varphi_B}$. Furthermore, ε is the diffuse interface thickness and $\frac{\varepsilon^2}{2}|\nabla\varphi|^2$ is a surface tension term which ensures a smooth transition between the two pure states. Finally, F is a double-well potential which favors phase separation.

Once the free energy is defined, the phase separation can be described as a gradient flow (see, for instance [23]),

$$\frac{\partial\varphi}{\partial t} = \Delta\mu, \quad \mu := \frac{\partial\mathcal{E}_{\mathrm{CH}}}{\partial\varphi} = f(\varphi) - \varepsilon^2\Delta\varphi,$$

where μ is the chemical potential and $f = F'$.

This corresponds to the well-known Cahn–Hilliard equation which plays an important role in Materials Science. In particular, phase separation phenomena play an essential role in the mechanical properties of an alloy (for instance, its strength). We refer the reader to, *e.g.*, [8, 9, 37, 39, 42] for more details.

It is worth recalling that Cahn–Hilliard type equations are also relevant in other contexts, namely, the ones in which phase separation and coarsening/clustering processes can be observed or come into play. We can mention, for instance, population dynamics [15], bacterial films [36], wound healing and tumor growth [10, 22, 35], thin films [46, 49], image processing and inpainting [6, 11–14, 19, 48], and even the rings of Saturn [50] and the clustering of mussels [38].

1.2. Nonlocal Cahn–Hilliard equation

1.2.1. Giacomin and Lebowitz model

The purely phenomenological derivation of the Cahn–Hilliard equation is somehow unsatisfactory from a physical point of view. This led G. Giacomin and J.L. Lebowitz to consider the problem of phase separation from a microscopic point of view, using a statistical mechanics approach (see [26]). Performing the hydrodynamic limit, they deduced a continuum model which is a nonlocal version of the Cahn–Hilliard equation. This model is characterized by the following Helmholtz free energy functional

$$\mathcal{E}_{n\mathrm{CH1}}(\varphi) = -\frac{1}{2}\int_\Omega\int_\Omega J(x-y)\varphi(x)\varphi(y)\,\mathrm{d}x\,\mathrm{d}y + \int_\Omega S(\varphi(x))\,\mathrm{d}x, \tag{1.2}$$

where $J : \mathbb{R}^N \to \mathbb{R}$ is a smooth convolution kernel such that $J(x) = J(-x)$. Furthermore, the convex potential S here is defined as follows:

$$S(s) = (s+1)\ln(s+1) + (1-s)\ln(1-s), \quad s \in]-1, 1[. \tag{1.3}$$

This potential is usually approximated by a convex polynomial. In that case, the nonlocal version of the Cahn–Hilliard system reads

$$\frac{\partial\varphi}{\partial t} = \Delta\mu, \quad \mu := \frac{\partial\mathcal{E}_{n\mathrm{CH1}}}{\partial\varphi} = f(\varphi) - J \star_\Omega \varphi, \tag{1.4}$$

where

$$(J \star_\Omega \varphi)(x,t) = \int_\Omega J(x-y)\varphi(y,t)\,\mathrm{d}y, \quad x \in \Omega, t \geq 0.$$

We refer the reader to the recent paper [25] (see addition in the references) for a rather complete theoretical picture.

1.2.2. Bates and Han model

On the other hand, P.W. Bates and J. Han in [3, 4] proposed the following nonlocal version of the Cahn–Hilliard energy

$$\mathcal{E}_{n\mathrm{CH2}}(\varphi) = \frac{1}{4}\int_\Omega\int_\Omega J(x-y)(\varphi(x)-\varphi(y))^2\,\mathrm{d}x\,\mathrm{d}y + \int_\Omega F(\varphi(x))\,\mathrm{d}x, \tag{1.5}$$

where F is the double-well potential as in the classical Cahn–Hilliard model (non convex potential), which is usually approximated by a smooth double-well potential of the form

$$F(s) = \frac{s^4}{4} + \frac{\gamma_1 - \gamma_2}{2} s^2, \quad \forall s \in \mathbb{R}, \tag{1.6}$$

where $\gamma_i, i = 1, 2$ are nonnegative constants. Here $\gamma_1 - \gamma_2 < 0$. However, note that, up to the constants, if $\gamma_1 - \gamma_2 > 0$ then F can be seen as a smooth approximation of S.

1.2.3. Combined models

On account of (1.2) and (1.5), we introduce the following energy, for $\alpha \in \{0, 1\}$,

$$\begin{aligned}\mathcal{E}_{n\mathrm{CH}}(\varphi) = \frac{1}{4} \int_\Omega \int_\Omega J(x-y) \left(\varphi(x) - \varphi(y)\right)^2 \, \mathrm{d}x \, \mathrm{d}y \\ + \frac{\alpha - 1}{2} \int_\Omega \int_\Omega J(x-y) (\varphi(x))^2 \, \mathrm{d}x \, \mathrm{d}y + \int_\Omega F(\varphi(x)) \, \mathrm{d}x,\end{aligned} \tag{1.7}$$

where F is given by (1.6). If $\alpha = 0$ and $\gamma_1 - \gamma_2 > 0$ then the energy can be viewed as an approximation of (1.2), while if $\alpha = 1$ and $\gamma_1 - \gamma_2 < 0$ then we obtain (1.5). Therefore, we consider

$$\frac{\partial \varphi}{\partial t} = \Delta \mu, \quad \mu := \frac{\partial \mathcal{E}_{n\mathrm{CH}}}{\partial \varphi} = \alpha (J \star_\Omega 1) \varphi + f(\varphi) - J \star_\Omega \varphi, \tag{1.8}$$

which can be rewritten as the following convective nonlocal and nonlinear diffusion equation:

$$\frac{\partial \varphi}{\partial t} = \nabla \cdot \left(\left(f'(\varphi) + \alpha \left(J \star_\Omega 1 \right) \right) \nabla \varphi \right) + \alpha \nabla \cdot \left(\left(\nabla J \star_\Omega 1 \right) \varphi \right) - \nabla \cdot \left(\nabla J \star_\Omega \varphi \right). \tag{1.9}$$

The term $[f'(\varphi) + \alpha J \star_\Omega 1]$ is referred to as the diffusive mobility, or simply the diffusivity. We assume that (1.8) is strictly non-degenerate, that is, there exists some $a > 0$ such that

$$f'(s) + \alpha \left(J \star_\Omega 1 \right)(x) \geqslant a > 0, \quad \text{a.a.} \quad x \in \Omega, \quad \forall s \in \mathbb{R}. \tag{1.10}$$

Observe that $J \star_\Omega 1$ is not necessarily constant unless we work with a periodic domain.

Remark 1.1. Note that (1.10) can be written as

$$\exists \, a > 0 \text{ such that } \left(J \star_\Omega 1 \right)(x) \geqslant \frac{a}{\alpha} + \frac{1}{\alpha} \max_{s \in \mathbb{R}} (-f'(s)), \quad \text{a.a.} \quad x \in \Omega.$$

Referring to (1.6), this assumption can be seen as

$$\exists \, b > 0 \text{ such that } \left(J \star_\Omega 1 \right)(x) \geqslant b, \quad \text{a.a.} \quad x \in \Omega. \tag{1.11}$$

Let Ω be such that $\partial\Omega$ satisfies the interior cone condition, namely, there exists an angle $\beta > 0$ and $r > 0$ such that, for each point $x \in \partial\Omega$, there exists a rotation $R \in SO(N)$ such that

$$(x + RC_\beta) \cap \mathcal{B}_r(x) \subset \overline{\Omega},$$

where C_β is the cone of opening angle β, that is,

$$C_\beta = \left\{ x \in \mathbb{R}^N ; x \cdot e_1 \leqslant |x| \cos\left(\frac{\beta}{2}\right) \right\}.$$

Assume that J is either $\frac{1}{\varepsilon^N}$ times the indicator function of the ball of radius ε or it behaves like a gaussian kernel of standard deviation ε, that is,

$$\exists \, C > 0 \text{ such that } \frac{1}{C} \frac{1}{\varepsilon^{\frac{N}{2}}} e^{-\frac{1}{C}\left(\frac{|x|}{\varepsilon}\right)^2} \leqslant J(x) \leqslant C \frac{1}{\varepsilon^{\frac{N}{2}}} e^{C\left(\frac{|x|}{\varepsilon}\right)^2}.$$

Then (1.11) holds, provided that $\partial\Omega$ satisfies the interior cone condition for a suitable β.

1.2.4. Cahn–Hilliard–Oono model

A further example of a nonlocal Cahn–Hilliard equation is obtained by considering the following Ohta–Kawasaki free energy

$$\mathcal{E}_{\mathrm{CHO}}(\varphi) = \frac{\varepsilon^2}{2}\int_\Omega |\nabla\varphi|^2\,\mathrm{d}x + \int_\Omega F(\varphi)\,\mathrm{d}x + \frac{\sigma}{2}\int_\Omega\int_\Omega G(x-y)\,(\varphi(x)-\langle\varphi\rangle)\,(\varphi(y)-\langle\varphi\rangle)\,\mathrm{d}x\,\mathrm{d}y, \tag{1.12}$$

where G describes the long-range interactions and $\sigma > 0$. In particular, in Oono's model (see [45], *cf.* also [51]), G is the Green function associated with the Laplace operator (up to a multiplicative constant). When the problem is associated with Neumann (or periodic) boundary conditions, we have (see [43])

$$-\Delta G(x-y) = \delta(x-y) - \frac{1}{\mathrm{meas}(\Omega)} \quad \text{in} \quad \Omega, \qquad \int_\Omega G\,\mathrm{d}x = 0. \tag{1.13}$$

Setting

$$\langle\varphi\rangle = \frac{1}{\mathrm{meas}(\Omega)}\int_\Omega \varphi\,\mathrm{d}x,$$

the gradient flow for this energy can be derived exactly as for the Cahn–Hilliard equation, namely,

$$\frac{\partial\varphi}{\partial t} = \Delta\frac{\partial\mathcal{E}_{\mathrm{CHO}}}{\partial\varphi},$$

which is equivalent to

$$\frac{\partial\varphi}{\partial t} + \sigma\,(\varphi - \langle\varphi\rangle) = \Delta\mu, \quad \mu = -\varepsilon^2\Delta\varphi + f(\varphi).$$

A more general form of the above equation is given by

$$\frac{\partial\varphi}{\partial t} + \sigma(\varphi - m) = \Delta\mu, \quad \mu = -\varepsilon^2\Delta\varphi + f(\varphi),$$

where m is real constant.

If $m = \langle\varphi\rangle$, then the mass is conserved. However, m can be a constant which is not necessarily equal to the spatial average of the initial datum. This is the so-called off-critical case and the total mass is conserved only asymptotically. Indeed, in that case we have, for all $t \in [0,T]$,

$$\langle\varphi\rangle = m + e^{-\sigma t}\,(\langle\varphi_0\rangle - m)\,. \tag{1.14}$$

This equation is known as the Cahn–Hilliard–Oono equation and was introduced to model long-range interactions; actually, this equation was also proposed in order to simplify numerical simulations (see [45]). Short-range interactions tend to homogenize the system, whereas long-range ones penalize the formation of too large structures; the competition between these two effects translates into the formation of a micro-separated state (also called super-crystal) with a spatially modulated order parameter, defining structures with a certain length scale at which modulation happens mostly (see [51] for more details and references). Note that the long-range interactions are repulsive when $\varphi(x)$ and $\varphi(y)$ have opposite signs and thus favor the formation of interfaces (see [51] and the references therein). For theoretical results see [27, 41] and the references therein (see also [2] for numerical results in the conserved case).

1.3. Our problem

Taking the previous models into account, here we consider the following initial and boundary value problem:

$$\begin{cases} \dfrac{\partial \varphi}{\partial t} + \nabla \cdot (u\varphi) + \sigma\left(\langle\varphi\rangle - m\right) = \Delta\mu + g, & \text{in} \quad \Omega \times (0,T), \\ \mu = \left(J \star_\Omega 1\right)\varphi - J \star_\Omega \varphi + f(\varphi) + \sigma G \star_\Omega \left(\varphi - \langle\varphi\rangle\right), & \text{in} \quad \Omega \times (0,T), \\ \dfrac{\partial \mu}{\partial n} = 0, & \text{on} \quad \partial\Omega \times (0,T), \\ \varphi(0) = \varphi_0, & \text{in} \quad \Omega, \end{cases} \tag{1.15}$$

where G is the Green function defined in (1.13). The system $(1.15)_1$–$(1.15)_2$ is the nonlocal version of the Cahn–Hilliard–Oono equation with a transport term which accounts for a possible flow of the mixture at a certain given velocity field u and an external source g. We must note that in our case the free energy is not necessarily decreasing unless we are not in the off-critical case and the velocity field vanishes.

This equation was studied in [18] (see also its references). In particular, well-posedness and existence of the global attractor were established. Furthermore, well-posedness results for (1.15) with singular potential and a degenerate mobility were obtained in [40].

Here we shall study the case $\alpha = 1$. The case $\alpha = 0$, with (1.3), will be considered elsewhere.

Remark 1.2. Integrating $(1.15)_1$ over Ω we find

$$\frac{\mathrm{d}}{\mathrm{d}t}\langle\varphi\rangle + \sigma\langle\varphi\rangle = \sigma m + \langle g\rangle,$$

which yields, for $\sigma \neq 0$,

$$\langle\varphi\rangle = m + \frac{1}{\sigma}\langle g\rangle + e^{-\sigma t}\left(\langle\varphi_0\rangle - m\right).$$

As far as the classical nonlocal Cahn–Hilliard equation is concerned (*i.e.*, $u = 0$, $g = 0$ and $\sigma = 0$), very few results dedicated to numerical simulations, or numerical methods, are available. The authors in [1] consider an implicit-explicit time stepping framework for a nonlocal system modeling turbulence, where, as in the present article, the nonlocal term is treated explicitly. Furthermore, the finite element approximation (in space) of nonlocal peridynamic equations with various boundary conditions is addressed in [52] (*cf.* [20] for a review). In addition, a finite difference method for the nonlocal Allen–Cahn equation with non-periodic boundary conditions is applied and analyzed in [5]. The work in [32] uses a spectral-Galerkin method to solve a nonlocal Allen–Cahn equation, but with a stochastic noise term and an equation modeling heat flow. For other articles dealing with approximating solutions to the nonlocal Cahn–Hilliard equation, see [24,34,47]. Finally, the authors in [29,30] study the nonlocal Cahn–Hilliard equation with periodic boundary conditions and finite difference discretizations in space. Recently, stronger convergence results of convex splitting schemes for the periodic nonlocal Allen–Cahn and Cahn–Hilliard equations have been obtained in [31].

In this article we give a first order in time numerical scheme for problem (1.15), derived from a convex splitting of the nonlocal energy. In particular, we show the stability of the scheme and the convergence to the exact solution. We also give two-dimensional numerical simulations that confirm our theoretical results and demonstrate the efficiency of our scheme. It should be noted here that the numerical computations of the nonlocal terms are particularly heavy: computing the nonlocal terms at every iteration thus becomes very difficult when the mesh discretization is small. To overcome this, we consider, in the numerical simulations, a rectangular domain Ω and we use the Discrete Fast Fourier Transformation (DFFT) function to compute the nonlocal terms.

2. Preliminaries

2.1. Notation

We denote by $((\cdot,\cdot))$ the usual L^2-scalar product, with associated norm $\|\cdot\|$. We further set $\|\cdot\|_* = \|(-\Delta)^{-\frac{1}{2}}\cdot\|$, where $(-\Delta)^{-1}$ denotes the inverse minus Laplace operator associated with Neumann boundary conditions and acting on functions with null spatial average. More generally, $\|\cdot\|_X$ denotes the norm of the real Banach space X.

We further denote by $\langle v\rangle$ the spatial average of a function $v \in L^1(\Omega)$, namely,

$$\langle v\rangle = \frac{1}{\mathrm{meas}(\Omega)}\,\langle v, 1\rangle_{(H^1(\Omega))^*,H^1(\Omega)}\,.$$

Therefore, the norm

$$\left(\|v - \langle v\rangle\|_*^2 + \langle v\rangle^2\right)^{\frac{1}{2}}$$

is equivalent to the usual norm of $(H^1(\Omega))^*$.

2.2. Assumptions

We make the following assumptions:

(A1) $\Omega \subset \mathbb{R}^N$, $N \leq 3$, is a bounded domain with a smooth boundary.
(A2) $J : \mathbb{R}^N \to \mathbb{R}$ satisfies $J = J_1 - J_2$, where J_1, J_2 are nonnegative functions in $\mathcal{W}^{1,1}(\mathbb{R}^N)$.
(A3) J_1 and J_2 are even, *i.e.*, $J_i(-x) = J_i(x)$, $\forall x \in \mathbb{R}^N$, $i = 1, 2$.
(A4) $f'(s) + (J \star_\Omega 1)(x) \geqslant a > 0$, a.a. $x \in \Omega$, $\forall s \in \mathbb{R}$.
(A5) $G : \mathbb{R}^N \to \mathbb{R}$ is the Green function (*cf.* (1.13)).
(A6) σ is a nonnegative constant.
(A7) m is a given constant.
(A8) $u \in (L^\infty(\Omega) \cap H_0^1(\Omega))^N$.
(A9) $g \in (H^1(\Omega))^*$.

We now state the existence and uniqueness of a weak solution (see [18]).

Proposition 2.1. *Let (A1)–(A9) hold. Let $\varphi_0 \in L^2(\Omega)$ be such that $F(\varphi_0) \in L^1(\Omega)$. Then, for every $T > 0$, there exists a unique weak solution φ to problem (1.15) on $[0, T]$ such that*

$$\varphi \in L^\infty(0, T; L^2(\Omega)) \cap L^2(0, T; H^1(\Omega)).$$

Remark 2.2. In the sequel for some results, we will require a higher regularity of the solution. To achieve that, the initial datum should be more regular as well as the interaction kernel J. For details the reader is referred to [3] where the existence of a classical solution is established (see also [25] for the singular potential case). In particular, the boundedness of solution can also be proven for smooth potentials. The presence of an additional linear reaction term does not affect the regularity results.

2.3. Convex energy splitting

Note that the physical range of the phase-field variable is $[-1, 1]$. Replacing the original potential with one whose growth is quadratic outside $[-1, 1]$ is a common modification in the literature (see, *e.g.*, [7, 44]). When the logarithmic potential is approximated by, *e.g.*, (1.6), one cannot ensure that the solutions take values in the physical range. However, also thanks to their global boundedness (which can be proven), numerical simulations available in the literature show that eventually the solution to the equation with the approximated potential takes its values in the interval $[-1, 1]$ where the two potentials coincide. Here we give in Section 4 (*cf.* Fig. 7)

some numerical evidences illustrating that the solutions with the double well potential or with its quadratic approximation are indeed quite similar. More precisely, in place of (1.6) we will take the following:

$$F(s) = \begin{cases} \dfrac{3+\gamma_1-\gamma_2}{2}(s+1)^2 + (\gamma_2-\gamma_1-1)(s+1) + \dfrac{1}{4} + \dfrac{\gamma_1-\gamma_2}{2}, & s < -1 \\ \dfrac{1}{4}s^4 + \dfrac{\gamma_1-\gamma_2}{2}s^2, & |s| \le 1, \\ \dfrac{3+\gamma_1-\gamma_2}{2}(s-1)^2 - (\gamma_2-\gamma_1-1)(s-1) + \dfrac{1}{4} + \dfrac{\gamma_1-\gamma_2}{2}, & s > 1 \end{cases} \tag{2.1}$$

where γ_i, $i = 1, 2$, are nonnegative constants.

Note that (2.1) implies that $F \in C^2(\mathbb{R})$ and $f' = F''$ satisfies the following global bound:

$$|f'(s)| \le 3 + |\gamma_1 - \gamma_2|,$$

for all $s \in \mathbb{R}$, *i.e.*, f' is globally bounded.

We consider the following nonlocal energy:

$$\begin{aligned} \mathcal{E}(\varphi) = & \int_\Omega F(\varphi)\,\mathrm{d}x + \frac{1}{4}\int_\Omega\int_\Omega J(x-y)(\varphi(x)-\varphi(y))^2\,\mathrm{d}x\,\mathrm{d}y \\ & + \frac{\sigma}{2}\int_\Omega\int_\Omega G(x-y)(\varphi(x)-\langle\varphi\rangle)(\varphi(y)-\langle\varphi\rangle)\,\mathrm{d}x\,\mathrm{d}y, \end{aligned} \tag{2.2}$$

where F is given by (2.1).

For $\sigma = 0$ in (2.2), we obtain energy (1.7) which can be related to the (local) Ginzburg–Landau energy (1.1). This relationship between the local and nonlocal energies can formally be obtained by using a Taylor expansion. In particular, noting that $(\varphi(x) - \varphi(y)) \approx (x-y)\cdot\nabla\varphi(x)$ we find that

$$\frac{1}{4}\int_\Omega\int_\Omega J(x-y)(\varphi(x)-\varphi(y))^2\,\mathrm{d}x\,\mathrm{d}y \approx \frac{1}{4}\int_\Omega\int_\Omega J(x-y)((x-y)\cdot\nabla\varphi(x))^2\,\mathrm{d}x\,\mathrm{d}y.$$

Using Fubini's theorem, we obtain an anisotropic version of the Dirichlet energy of φ. This argument is just formal but it underlines the link with the original (local) model. However, it is interesting to note that it can be made rigorous by taking

$$J_\varepsilon(x-y) = \frac{\varrho_\varepsilon(x-y)}{|x-y|^2},$$

where ϱ_ε is a family of radial mollifier, and letting ε go to 0 (see [16]). Concerning non-singular (*e.g.*, smooth) kernels, like in the present case, we refer the reader to the recent contribution [16].

From assumptions (A3) and (A5), we can rewrite (2.2) in the following form:

$$\begin{aligned} \mathcal{E}(\varphi) = & \frac{1}{2}\left(((J\star_\Omega 1)\varphi,\varphi) + (F(\varphi),1)\right) - \frac{1}{2}(J\star_\Omega\varphi,\varphi) \\ & + \frac{\sigma}{2}(G\star_\Omega(\varphi-\langle\varphi\rangle),(\varphi-\langle\varphi\rangle)). \end{aligned} \tag{2.3}$$

Besides that, using $J = J_1 - J_2$, the last two terms in (2.2) can be written as

$$\begin{aligned} & \frac{1}{4}\int_\Omega\int_\Omega J(x-y)(\varphi(x)-\varphi(y))^2\,\mathrm{d}x\,\mathrm{d}y + \frac{\sigma}{2}\int_\Omega\int_\Omega G(x-y)(\varphi(x)-\langle\varphi\rangle)(\varphi(y)-\langle\varphi\rangle)\,\mathrm{d}x\,\mathrm{d}y \\ & \quad = \frac{1}{4}\int_\Omega\int_\Omega J_1(x-y)(\varphi(x)-\varphi(y))^2\,\mathrm{d}x\,\mathrm{d}y + \frac{1}{4}\int_\Omega\int_\Omega J_2(x-y)(\varphi(x)-\varphi(y))^2\,\mathrm{d}x\,\mathrm{d}y \\ & \qquad + \frac{\sigma}{2}\int_\Omega\int_\Omega G(x-y)(\varphi(x)-\langle\varphi\rangle)(\varphi(y)-\langle\varphi\rangle)\mathrm{d}x\,\mathrm{d}y. \end{aligned}$$

Thus, expanding the square $(\varphi(x)-\varphi(y))^2$ and completing the square of $(\varphi(x)-\langle\varphi\rangle)(\varphi(y)-\langle\varphi\rangle)$ in the first term and the last one of the last equality, respectively, we get

$$\begin{aligned}
&\frac{1}{4}\int_\Omega\int_\Omega J_1(x-y)(\varphi(x))^2\,\mathrm{d}x\,\mathrm{d}y+\frac{1}{4}\int_\Omega\int_\Omega J_1(x-y)(\varphi(y))^2\,\mathrm{d}x\,\mathrm{d}y\\
&\quad-\frac{1}{2}\int_\Omega\int_\Omega J_1(x-y)\varphi(x)\varphi(y)\,\mathrm{d}x\,\mathrm{d}y+\frac{1}{4}\int_\Omega\int_\Omega J_2(x-y)(\varphi(x)-\varphi(y))^2\,\mathrm{d}x\,\mathrm{d}y\\
&\quad+\frac{\sigma}{4}\int_\Omega\int_\Omega G(x-y)(\varphi(x)-\langle\varphi\rangle)^2\,\mathrm{d}x\,\mathrm{d}y+\frac{\sigma}{4}\int_\Omega\int_\Omega G(x-y)(\varphi(y)-\langle\varphi\rangle)^2\,\mathrm{d}x\,\mathrm{d}y\\
&\quad-\frac{\sigma}{4}\int_\Omega\int_\Omega G(x-y)(\varphi(x)-\varphi(y))^2\,\mathrm{d}x\,\mathrm{d}y,
\end{aligned}$$

which yields, owing to the symmetry of J_1, J_2, G,

$$\begin{aligned}
&\frac{1}{2}\int_\Omega\int_\Omega J_1(x-y)(\varphi(x))^2\,\mathrm{d}x\,\mathrm{d}y-\frac{1}{2}\int_\Omega\int_\Omega J_1(x-y)\varphi(x)\varphi(y)\,\mathrm{d}x\,\mathrm{d}y\\
&\quad-\frac{1}{4}\int_\Omega\int_\Omega J_2(x-y)(\varphi(x)-\varphi(y))^2\,\mathrm{d}x\,\mathrm{d}y-\frac{\sigma}{4}\int_\Omega\int_\Omega G(x-y)(\varphi(x)-\varphi(y))^2\,\mathrm{d}x\,\mathrm{d}y\\
&\quad+\frac{\sigma}{2}\int_\Omega\int_\Omega G(x-y)(\varphi(x)-\langle\varphi\rangle)^2\,\mathrm{d}x\,\mathrm{d}y.
\end{aligned}$$

Note now that

$$\begin{aligned}
-\frac{1}{4}\int_\Omega\int_\Omega J_1(x-y)(\varphi(x)+\varphi(y))^2\,\mathrm{d}x\,\mathrm{d}y=&-\frac{1}{2}\int_\Omega\int_\Omega J_1(x-y)(\varphi(x))^2\,\mathrm{d}x\,\mathrm{d}y\\
&-\frac{1}{2}\int_\Omega\int_\Omega J_1(x-y)\varphi(x)\varphi(y)\,\mathrm{d}x\,\mathrm{d}y,
\end{aligned}$$

where we have expanded the square and used the symmetry of J_1. Therefore,

$$\begin{aligned}
&\frac{1}{4}\int_\Omega\int_\Omega J(x-y)(\varphi(x)-\varphi(y))^2\,\mathrm{d}x\,\mathrm{d}y+\frac{\sigma}{2}\int_\Omega\int_\Omega G(x-y)(\varphi(x)-\langle\varphi\rangle)(\varphi(y)-\langle\varphi\rangle)\,\mathrm{d}x\,\mathrm{d}y\\
&\quad=-\frac{1}{4}\int_\Omega\int_\Omega J_1(x-y)(\varphi(x)+\varphi(y))^2\,\mathrm{d}x\,\mathrm{d}y-\frac{1}{4}\int_\Omega\int_\Omega J_2(x-y)(\varphi(x)-\varphi(y))^2\,\mathrm{d}x\,\mathrm{d}y\\
&\qquad+\int_\Omega\int_\Omega J_1(x-y)(\varphi(x))^2\,\mathrm{d}x\,\mathrm{d}y-\frac{\sigma}{4}\int_\Omega\int_\Omega G(x-y)(\varphi(x)-\varphi(y))^2\,\mathrm{d}x\,\mathrm{d}y\\
&\qquad+\frac{\sigma}{2}\int_\Omega\int_\Omega G(x-y)(\varphi(x)-\langle\varphi\rangle)^2\,\mathrm{d}x\,\mathrm{d}y.
\end{aligned}$$

We then deduce that

$$\begin{aligned}
&\frac{1}{4}\int_\Omega\int_\Omega J(x-y)(\varphi(x)-\varphi(y))^2\,\mathrm{d}x\,\mathrm{d}y+\frac{\sigma}{2}\int_\Omega\int_\Omega G(x-y)(\varphi(x)-\langle\varphi\rangle)(\varphi(y)-\langle\varphi\rangle)\,\mathrm{d}x\,\mathrm{d}y\\
&\quad=-\frac{1}{4}\int_\Omega\int_\Omega\Big[J_1(x-y)(\varphi(x)+\varphi(y))^2+(J_2(x-y)+\sigma G(x-y))(\varphi(x)-\varphi(y))^2\Big]\,\mathrm{d}x\,\mathrm{d}y\\
&\qquad+\int_\Omega\int_\Omega J_1(x-y)(\varphi(x))^2\,\mathrm{d}x\,\mathrm{d}y+\frac{\sigma}{2}\int_\Omega\int_\Omega G(x-y)(\varphi(x)-\langle\varphi\rangle)^2\,\mathrm{d}x\,\mathrm{d}y.
\end{aligned}$$

Consequently, a convex splitting of $\mathcal{E}$ is given by

$$\mathcal{E}(\varphi)=\mathcal{E}_1(\varphi)-\mathcal{E}_2(\varphi),$$

where

$$\begin{aligned}\mathcal{E}_1(\varphi) = &\int_\Omega\int_\Omega J_1(x-y)(\varphi(x))^2\,\mathrm{d}x\,\mathrm{d}y\\ &+\frac{\sigma}{2}\int_\Omega\int_\Omega G(x-y)(\varphi(x)-\langle\varphi\rangle)^2\,\mathrm{d}x\,\mathrm{d}y+\frac{c_1}{2}\int_\Omega(\varphi(x))^2\mathrm{d}x\end{aligned}\tag{2.4}$$

and

$$\begin{aligned}\mathcal{E}_2(\varphi) = &\frac{1}{4}\int_\Omega\int_\Omega\left[J_1(x-y)(\varphi(x)+\varphi(y))^2+(J_2(x-y)+\sigma G(x-y))(\varphi(x)-\varphi(y))^2\right]\mathrm{d}x\,\mathrm{d}y\\ &-\int_\Omega F(\varphi(x))\,\mathrm{d}x+\frac{c_1}{2}\int_\Omega(\varphi(x))^2\,\mathrm{d}x.\end{aligned}\tag{2.5}$$

Remark 2.3. If c_1 is large enough, it is easy to show that $\mathcal{E}_1$ and $\mathcal{E}_2$ are convex. Note that the choice (2.1) allows us to put a convex quadratic term in $\mathcal{E}_2$. Thus, we can handle this term explicitly (*i.e.*, we can avoid Newton's method). This simplifies the computational problems. As we noted above, this choice does not seem to affect the numerical simulations. In particular, if σ, u, and g vanish then we obtain numerical results which are comparable with the ones obtained in [29].

3. Numerical scheme: definitions and properties

As far as the Euler time discretization for this problem is concerned, the time step $\delta t > 0$ is fixed. The resulting time-stepping scheme reads

$$\frac{\varphi^{n+1}-\varphi^n}{\delta t}=\Delta\mu^{n+1},\quad \mu^{n+1}:=\frac{\partial\mathcal{E}_1}{\partial\varphi}(\varphi^{n+1})-\frac{\partial\mathcal{E}_2}{\partial\varphi}(\varphi^n).$$

This translates into a numerical scheme of the form ($(1.15)_1$ and $(1.15)_2$)

$$\begin{aligned}\frac{1}{\delta t}\left(\varphi^{n+1}-\varphi^n\right)&=\Delta\mu^{n+1},\\ \mu^{n+1}&=2\left(J_1\star_\Omega 1\right)\varphi^{n+1}+c_1\left(\varphi^{n+1}-\varphi^n\right)+f(\varphi^n)\\ &\quad-\left(J_1\star_\Omega 1+J_2\star_\Omega 1\right)\varphi^n+\sigma\left(G\star_\Omega 1\right)\left(\varphi^{n+1}-\varphi^n\right)+\sigma G\star_\Omega\left(\varphi^n-\langle\varphi^n\rangle\right)-J\star_\Omega\varphi^n.\end{aligned}$$

where $f(\varphi^n)=F'(\varphi^n)$. Using the properties of the Green function G when the problem is endowed with no-flux boundary conditions (see (1.13)), the scheme can be rewritten as follows

$$\begin{aligned}\frac{1}{\delta t}(\varphi^{n+1}-\varphi^n)+\sigma(\varphi^n-\langle\varphi^n\rangle)&=\Delta\mu^{n+1},\\ \mu^{n+1}&=2(J_1\star_\Omega 1)\varphi^{n+1}+c_1(\varphi^{n+1}-\varphi^n)+f(\varphi^n)\\ &\quad-(J_1\star_\Omega 1+J_2\star_\Omega 1)\varphi^n-J\star_\Omega\varphi^n.\end{aligned}$$

More generally, we replace $\langle\varphi^n\rangle$ by a real constant m which is not necessarily equal to the spatial average of the initial datum since we are interested to take the off-critical case into account. So we have the following numerical scheme:

$$\begin{aligned}\frac{1}{\delta t}(\varphi^{n+1}-\varphi^n)+\sigma(\varphi^n-m)&=\Delta\mu^{n+1},\\ \mu^{n+1}&=2(J_1\star_\Omega 1)\varphi^{n+1}+c_1(\varphi^{n+1}-\varphi^n)+f(\varphi^n)\\ &\quad-(J_1\star_\Omega 1+J_2\star_\Omega 1)\varphi^n-J\star_\Omega\varphi^n.\end{aligned}$$

Finally, we add a transport term which models a possible flow of the mixture at a certain given velocity field u, that is, the scheme reads

$$\frac{1}{\delta t}(\varphi^{n+1}-\varphi^n)+\sigma(\varphi^n-m)+\nabla\cdot(u\varphi^{n+1})=\Delta\mu^{n+1}+g, \tag{3.1}$$

$$\begin{aligned}\mu^{n+1}&=2(J_1\star_\Omega 1)\varphi^{n+1}+c_1(\varphi^{n+1}-\varphi^n)+f(\varphi^n)\\&\quad-(J_1\star_\Omega 1+J_2\star_\Omega 1)\varphi^n-J\star_\Omega\varphi^n.\end{aligned} \tag{3.2}$$

for a given external source g.

3.1. Consistency of the scheme

Let $\varphi_n=\varphi(x,n\delta t)$ be the exact solution of (1.15) at time $n\delta t$, where φ is the exact solution. Then we have the following.

Proposition 3.1. *Let (A1)–(A9) hold. Let $\varphi_0\in H^3(\Omega)$ satisfies the compatibility condition $\frac{\partial\mu}{\partial\nu}=0$ a.e. on $\partial\Omega$. In addition, suppose that $\|\frac{\partial^2\varphi}{\partial t^2}(\cdot)\|$ and $\|\frac{\partial\varphi}{\partial t}(\cdot)\|_{H^1(\Omega)}$ are continuous with respect to time. Then, the numerical scheme (3.1) and (3.2) is consistent with the continuous equation (1.15) and is of order one in time. This yields that the local truncation error of the scheme, defined as (see [48] for instance):*

$$\begin{aligned}\tau_n(\delta t)&=\frac{1}{\delta t}(\varphi_{n+1}-\varphi_n)-c_1\Delta(\varphi_{n+1}-\varphi_n)-2\Delta((J_1\star_\Omega 1)\varphi_{n+1})\\&\quad-\Delta(f(\varphi_n))+\sigma(\varphi_n-m)+\Delta((J_1\star_\Omega 1+J_2\star_\Omega 1)\varphi_n)\\&\quad+\Delta(J\star_\Omega\varphi_n)+\nabla\cdot(u\varphi_{n+1})-g,\end{aligned} \tag{3.3}$$

satisfies

$$\|\tau_n\|_{(H^1(\Omega))^*}=O(\delta t),\quad \text{as}\quad \delta t\to 0.$$

Furthermore, the global truncation error of the scheme satisfies

$$\tau(\delta t)=\max_n\|\tau_n\|_{(H^1(\Omega))^*}=O(\delta t),\quad \text{as}\quad \delta t\to 0.$$

Proof. First, observe (from (1.15), $\alpha=1$) that

$$\begin{aligned}&-\frac{\partial\varphi}{\partial t}(n\delta t)+2\Delta((J_1\star_\Omega 1)\varphi_n)-\nabla\cdot(u\varphi_n)\\&\quad=\sigma(\varphi_n-m)-\Delta((J\star_\Omega 1)\varphi_n)+\Delta(J\star_\Omega\varphi_n)-\Delta f(\varphi_n)+2\Delta((J_1\star_\Omega 1)\varphi_n)-g\\&\quad=\sigma(\varphi_n-m)+\Delta(J\star_\Omega\varphi_n)+\Delta((J_1\star_\Omega 1+J_2\star_\Omega 1)\varphi_n)-\Delta f(\varphi_n)-g.\end{aligned}$$

Therefore, the local truncation error $\tau_n(\delta t)$ is given by

$$\begin{aligned}\tau_n(\delta t)&=\frac{1}{\delta t}(\varphi_{n+1}-\varphi_n)-c_1\Delta(\varphi_{n+1}-\varphi_n)-2\Delta((J_1\star_\Omega 1)(\varphi_{n+1}-\varphi_n))\\&\quad+\nabla\cdot(u(\varphi_{n+1}-\varphi_n))-\frac{\partial\varphi}{\partial t}(n\delta t).\end{aligned} \tag{3.4}$$

Integrating (3.4) over Ω, we obtain

$$\langle\tau_n(\delta t)\rangle=\left\langle\frac{1}{\delta t}(\varphi_{n+1}-\varphi_n)-\frac{\partial\varphi}{\partial t}(n\delta t)\right\rangle$$

and by using standard Taylor expansion arguments and the boundedness of $\left\langle \frac{\partial^2 \varphi}{\partial t^2}(\cdot) \right\rangle$, it is easy to show that

$$\langle \tau_n(\delta t) \rangle = O(\delta t). \tag{3.5}$$

On the other hand, we can rewrite the local truncation error $\tau_n(\delta t)$ as follows:

$$\tau_n = \tau_n^1(\delta t) + \tau_n^2(\delta t), \quad \text{where}$$
$$\tau_n^1(\delta t) = \frac{1}{\delta t}(\varphi_{n+1} - \varphi_n) - \frac{\partial \varphi}{\partial t}(n\delta t)$$

and

$$\tau_n^2(\delta t) = -2\Delta((J_1 \star_\Omega 1)(\varphi_{n+1} - \varphi_n)) + \nabla \cdot (u(\varphi_{n+1} - \varphi_n)) - c_1 \Delta(\varphi_{n+1} - \varphi_n).$$

By using standard Taylor expansion arguments and the boundedness of $\| \frac{\partial^2 \varphi}{\partial t^2}(\cdot) \|$, it is easy to show that

$$\|\tau_n^1\| = O(\delta t).$$

Owing to the last equality, (3.5), and the continuous embedding from $(H^1(\Omega))^*$ to $L^2(\Omega)$, we then have

$$\|\tau_n^1\|_{(H^1(\Omega))^*} = O(\delta t).$$

Moreover, writing

$$\varphi_{n+1} = \varphi_n + \delta t \frac{\partial \varphi}{\partial t}(t^*), \quad t_\Omega^\star \in (n\delta t, (n+1)\delta t),$$

we have

$$\tau_n^2 = -2\delta t \Delta \left((J_1 \star_\Omega 1) \frac{\partial \varphi}{\partial t}(t^*) \right) + \delta t \nabla \cdot \left(u \frac{\partial \varphi}{\partial t}(t^*) \right) - c_1 \delta t \Delta \frac{\partial \varphi}{\partial t}(t^*)$$

and

$$(-\Delta)^{-\frac{1}{2}} \tau_n^2 = -2\delta t (-\Delta)^{\frac{1}{2}} (J_1 \star_\Omega 1) \frac{\partial \varphi}{\partial t}(t^*) - \delta t \left(u \frac{\partial \varphi}{\partial t}(t^*) \right) - c_1 \delta t (-\Delta)^{\frac{1}{2}} \frac{\partial \varphi}{\partial t}(t^*).$$

Thus, we get

$$\|\tau_n^2\|_* \leqslant c\, \delta t \left[\left\| \nabla \left((J_1 \star_\Omega 1) \frac{\partial \varphi}{\partial t}(t^*) \right) \right\| + \left\| u \frac{\partial \varphi}{\partial t}(t^*) \right\| + c_1 \left\| \nabla \frac{\partial \varphi}{\partial t}(t^*) \right\| \right].$$

Hence we have

$$\left\| \tau_n^2(\delta t) \right\|_* \leqslant c\, \delta t \left(\left\| \frac{\partial \varphi}{\partial t}(t^*) \right\|^2 + \left\| \nabla \frac{\partial \varphi}{\partial t}(t^*) \right\|^2 + \left\| \frac{\partial \varphi}{\partial t}(t^*) \right\|_{H^1(\Omega)}^2 \right),$$

which yields, owing to (3.5),

$$\|\tau_n^2(\delta t)\|_{(H^1(\Omega))^*} = O(\delta t), \quad \text{as} \quad \delta t \to 0,$$

and

$$\tau = \max_n \|\tau_n\|_{(H^1(\Omega))^*} = O(\delta t), \quad \text{as} \quad \delta t \to 0.$$

□

3.2. Solvability and stability of the scheme

Assume that $u \equiv g \equiv 0$ and $\sigma = 0$. Then, it can be shown that the convex splitting framework automatically confers unconditional solvability and stability properties to our scheme (see [21]). We now assume that $u,\ g \not\equiv 0$ and $\sigma > 0$. The solvability follows immediately from the fact that $\mathcal{E}_2$ is convex, see [21].

On account of (2.1), the stability of the scheme is stated and proved here below.

Theorem 3.2. *Let φ^n be the n-th iterate of (3.1) and (3.2). We assume that (A1)–(A9) are satisfied and that the kernel J satisfies*

$$0 < \beta = 3 + |\gamma_1 - \gamma_2| < J \star_\Omega 1, \quad \text{a.e.} \quad \text{in} \quad \Omega. \tag{3.6}$$

Then, for any $0 < T < \infty$ provided δt is sufficiently small, the sequence φ^l with $l \in \mathbb{N}$ such that $l \leqslant \frac{T}{\delta t}$ is bounded in $L^2(\Omega)$, i.e.,

$$\max_{0 \leqslant l \leqslant T/\delta t} \|\varphi^l\|^2 + \ \delta t \|\nabla \varphi^l\|^2 \leqslant C,$$

where C is a constant which only depends on N, T, Ω, β, σ, J, g, u, and on the initial conditions.

Remark 3.3. Note that (3.6) is nothing but (A4) reformulated for the modified potential (2.1).

Proof. We have, owing to Young's inequality and testing (3.1) with $\psi = 2\delta t \varphi^{n+1}$,

$$\begin{aligned} &\|\varphi^{n+1}\|^2 - \|\varphi^n\|^2 + 2\delta t \left(\nabla \mu^{n+1}, \nabla \varphi^{n+1}\right) \\ &\quad \leqslant 2\delta t \left(u\varphi^{n+1}, \nabla \varphi^{n+1}\right) + 2\delta t \left(g, \varphi^{n+1}\right) - 2\sigma \delta t \left(\varphi^n - m, \varphi^{n+1}\right). \end{aligned} \tag{3.7}$$

Now, multiply (3.2) by $-2\delta t \Delta \varphi^{n+1}$ to obtain

$$\begin{aligned} 2\delta t(\nabla \mu^{n+1}, \nabla \varphi^{n+1}) &= 4\delta t(\nabla[(J_1 \star_\Omega 1)\varphi^{n+1}], \nabla \varphi^{n+1}) \\ &\quad + 2c_1 \delta t(\nabla \varphi^{n+1} - \nabla \varphi^n, \nabla \varphi^{n+1}) + 2\delta t(f'(\varphi^n)\nabla \varphi^n, \nabla \varphi^{n+1}) \\ &\quad - 2\delta t(\nabla[(J_1 \star_\Omega 1 + J_2 \star_\Omega 1)\varphi^n], \nabla \varphi^{n+1}) - 2\delta t(\nabla(J \star_\Omega \varphi^n), \nabla \varphi^{n+1}). \end{aligned} \tag{3.8}$$

Collecting (3.8), on account of (3.7), we infer

$$\begin{aligned} \|\varphi^{n+1}\|^2 - \|\varphi^n\|^2 \leqslant &- 2c_1 \delta t(\nabla \varphi^{n+1} - \nabla \varphi^n, \nabla \varphi^{n+1}) \\ &- 4\delta t(\nabla[(J_1 \star_\Omega 1)\varphi^{n+1}], \nabla \varphi^{n+1}) - 2\delta t(f'(\varphi^n)\nabla \varphi^n, \nabla \varphi^{n+1}) \\ &+ 2\delta t(\nabla[(J_1 \star_\Omega 1 + J_2 \star_\Omega 1)\varphi^n], \nabla \varphi^{n+1}) - 2\sigma \delta t((\varphi^n - m), \varphi^{n+1}) \\ &+ 2\delta t(\nabla(J \star_\Omega \varphi^n), \nabla \varphi^{n+1}) + 2\delta t((u\varphi^{n+1}, \nabla \varphi^{n+1}) + 2\delta t(g, \varphi^{n+1})) \\ = &\ \mathrm{I} + \mathrm{II} + \mathrm{III} + \mathrm{IV} + \mathrm{V} + \mathrm{VI} + \mathrm{VII} + \mathrm{VIII}. \end{aligned} \tag{3.9}$$

Applying Young's inequality, we have

$$\mathrm{I} \leqslant -c_1 \delta t \|\nabla \varphi^{n+1}\|^2 + c_1 \delta t \|\nabla \varphi^n\|^2, \tag{3.10}$$

and

$$\begin{aligned} \mathrm{II} = &- 4\delta t((J_1 \star_\Omega 1)\nabla \varphi^{n+1}, \nabla \varphi^{n+1}) \\ &- 4\delta t(\nabla(J_1 \star_\Omega 1)\varphi^{n+1}, \nabla \varphi^{n+1}) \\ \leqslant &- 4\delta t \int_\Omega (J_1 \star_\Omega 1)|\nabla \varphi^{n+1}|^2 \mathrm{d}x \\ &+ \frac{4}{\kappa} \delta t \|J_1\|^2_{W^{1,1}} \|\varphi^{n+1}\|^2 + \kappa \delta t \|\nabla \varphi^{n+1}\|^2, \end{aligned} \tag{3.11}$$

for all $\kappa > 0$. Furthermore, owing to assumption (3.6),

$$\mathrm{III} \leqslant \beta\delta t(\|\nabla\varphi^{n+1}\|^2 + \|\nabla\varphi^n\|^2). \tag{3.12}$$

Observe now that

$$\begin{aligned}\mathrm{IV} \leqslant{}& \delta t\int_\Omega (J_1 \star_\Omega 1 + J_2 \star_\Omega 1)|\nabla\varphi^{n+1}|^2\,\mathrm{d}x\\ &+ \delta t\int_\Omega (J_1 \star_\Omega 1 + J_2 \star_\Omega 1)|\nabla\varphi^{n}|^2\,\mathrm{d}x\\ &+ \frac{c}{\kappa}\delta t(\|J_1\|^2_{W^{1,1}} + \|J_2\|^2_{W^{1,1}})\|\varphi^n\|^2 + \kappa\delta t\|\nabla\varphi^{n+1}\|^2,\end{aligned} \tag{3.13}$$

for all $\kappa > 0$. Besides, we further have

$$\mathrm{V} \leqslant \sigma\delta t\|\varphi^n\|^2 + 2\sigma\delta t\|\varphi^{n+1}\|^2 + \sigma m^2\mathrm{meas}(\Omega)\delta t \tag{3.14}$$

and

$$\mathrm{VI} \leqslant \kappa\delta t\|\nabla\varphi^{n+1}\|^2 + \frac{\|J\|^2_{W^{1,1}}}{\kappa}\delta t\|\varphi^n\|^2, \tag{3.15}$$

for all $\kappa > 0$. Finally, using assumptions (A8) and (A9), we find

$$\mathrm{VII} \leqslant \kappa\delta t\|\nabla\varphi^{n+1}\|^2 + \frac{\|u\|^2_{L^\infty}}{\kappa}\delta t\|\varphi^{n+1}\|^2 \tag{3.16}$$

and

$$\begin{aligned}\mathrm{VIII} &\leqslant \kappa\delta t\|\nabla\varphi^{n+1}\|^2 + \frac{\|g - \langle g,1\rangle_{(H^1(\Omega))^*,H^1(\Omega)}\|^2_*}{\kappa}\delta t + 2c\delta t\,\langle g,1\rangle_{(H^1(\Omega))^*,H^1(\Omega)}\langle\varphi^{n+1}\rangle\\ &\leqslant \kappa\delta t\|\nabla\varphi^{n+1}\|^2 + \kappa\delta t\|\varphi^{n+1}\|^2 + c\frac{\|g - \langle g,1\rangle_{(H^1(\Omega))^*,H^1(\Omega)}\|^2_* + \langle g,1\rangle^2_{(H^1(\Omega))^*,H^1(\Omega)}}{\kappa}\delta t,\end{aligned} \tag{3.17}$$

for all $\kappa > 0$. Collecting (3.10)–(3.17), on account of (3.9), we infer

$$\begin{aligned}\|\varphi^{n+1}\|^2 - \|\varphi^n\|^2 + \delta t\int_\Omega \Big[c_1 + 4(J_1 \star_\Omega 1) - (J_1 \star_\Omega 1 + J_2 \star_\Omega 1) - \beta - 5\kappa\Big]|\nabla\varphi^{n+1}|^2\,\mathrm{d}x&\\ \leqslant \delta t\int_\Omega \Big[c_1 + (J_1 \star_\Omega 1 + J_2 \star_\Omega 1) + \beta\Big]|\nabla\varphi^n|^2\,\mathrm{d}x&\\ + \delta t\left(\frac{4\|J_1\|^2_{W^{1,1}}}{\kappa} + \frac{\|u\|^2_{L^\infty}}{\kappa} + \kappa + 2\sigma\right)\|\varphi^{n+1}\|^2&\\ + \delta t\left(\frac{c(\|J_1\|^2_{W^{1,1}} + \|J_2\|^2_{W^{1,1}})}{\kappa} + \frac{\|J\|^2_{W^{1,1}}}{\kappa} + \sigma\right)\|\varphi^n\|^2&\\ + \left(\sigma m^2\mathrm{meas}(\Omega) + \frac{\|g\|^2_{(H^1(\Omega))^*}}{\kappa}\right)\delta t.&\end{aligned} \tag{3.18}$$

Summing over n from $n=0$ to $n=l-1$, we have

$$\begin{aligned}\|\varphi^l\|^2 - \|\varphi^0\|^2 + \delta t \int_\Omega (2\zeta(x) - 5\kappa) \sum_{n=1}^{l-1} |\nabla\varphi^n|^2 \,\mathrm{d}x + \delta t \int_\Omega (\zeta(x) + 2(J_1 \star_\Omega 1) + c_1 - 5\kappa)|\nabla\varphi^l|^2 \,\mathrm{d}x \\ \leqslant \left(\frac{4\|J_1\|^2_{W^{1,1}}}{\kappa} + \frac{\|u\|^2_{L^\infty}}{\kappa} + \kappa + 2\sigma \right) \delta t \sum_{n=0}^{l-1} \|\varphi^{n+1}\|^2 \\ + \left(\frac{c\left(\|J_1\|^2_{W^{1,1}} + \|J_2\|^2_{W^{1,1}}\right)}{\kappa} + \frac{\|J\|^2_{W^{1,1}}}{\kappa} + \sigma \right) \delta t \sum_{n=0}^{l-1} \|\varphi^n\|^2 \\ + \left[\int_\Omega \left(c_1 + (J_1 \star_\Omega 1 + J_2 \star_\Omega 1) + \beta\right) |\nabla\varphi^0|^2 \,\mathrm{d}x \right. \\ \left. + \sigma m^2 \mathrm{meas}(\Omega) + \frac{\|g\|^2_{(H^1(\Omega))^*}}{\kappa} \right] l\delta t, \end{aligned} \tag{3.19}$$

with $\zeta(x) := (J \star_\Omega 1)(x) - \beta > 0$ for almost any $x \in \Omega$ according to (3.6). Hence, taking κ small enough such that $\frac{5}{2}\kappa < \zeta(x)$ for almost any $x \in \Omega$, we obtain

$$2\zeta(x) - 5\kappa > 0, \quad \text{for} \quad \text{a.a.} \quad x \in \Omega, \tag{3.20}$$

and

$$\begin{aligned}\eta(x) &:= c_1 + 4(J \star_\Omega 1) - (J_1 \star_\Omega 1 + J_2 \star_\Omega 1) - \beta - 5\kappa \\ &= \zeta(x) + 2(J_1 \star_\Omega 1) + c_1 - 5\kappa \\ &= 2\zeta(x) - 5\kappa + (J_1 \star_\Omega 1) + (J_2 \star_\Omega 1) + c_1 + \beta \geqslant 1, \quad \text{for} \quad \text{a.a.} \quad x \in \Omega. \end{aligned} \tag{3.21}$$

Setting

$$\begin{aligned} C_1 &= \frac{4\|J_1\|^2_{W^{1,1}}}{\kappa} + \frac{\|u\|^2_{L^\infty}}{\kappa} + \kappa + 2\sigma, \\ C_2 &= c\left(\frac{\|J_1\|^2_{W^{1,1}}}{\kappa} + \frac{\|J_2\|^2_{W^{1,1}}}{\kappa} \right) + \frac{\|J\|^2_{W^{1,1}}}{\kappa} + \sigma, \end{aligned}$$

and

$$C_3 = \sigma m^2 \mathrm{meas}(\Omega) + \frac{\|g\|^2_{(H^1(\Omega))^*}}{\kappa} + \int_\Omega \left(c_1 + (J_1 \star_\Omega 1 + J_2 \star_\Omega 1) + \beta\right) |\nabla\varphi^0|^2 \,\mathrm{d}x,$$

it thus follows from (3.19) to (3.21) that

$$\|\varphi^l\|^2 + \delta t \|\nabla\varphi^l\|^2 \leqslant C_1 \delta t \sum_{n=0}^{l-1} \|\varphi^{n+1}\|^2 + C_2 \delta t \sum_{n=0}^{l-1} \|\varphi^n\|^2 + C_3 l\delta t + \|\varphi^0\|^2, \tag{3.22}$$

whence, after some simplifications,

$$(1 - C_1\delta t)\|\varphi^l\|^2 + \delta t \|\nabla\varphi^l\|^2 \leqslant (C_1 + C_2)\delta t \sum_{n=1}^{l-1} \|\varphi^n\|^2 + (C_3 + C_2\|\varphi^0\|^2) l\delta t + \|\varphi^0\|^2. \tag{3.23}$$

Assuming that $\delta t < \frac{1}{2C_1}$ and $l\delta t \leqslant T$ and dividing the last inequality by $(1 - \delta t C_1)$, we arrive at

$$\|\varphi^l\|^2 + \delta t \|\nabla\varphi^l\|^2 \leqslant 2(C_1 + C_2)\delta t \sum_{n=1}^{l-1} \|\varphi^n\|^2 + 2T(C_3 + C_2\|\varphi^0\|^2) + 2\|\varphi^0\|^2. \tag{3.24}$$

An application of the discrete Gronwall's inequality yields the desired result and the proof is complete. □

3.3. Convergence to the exact solution

In this section, we establish the convergence of the discrete solution to the continuous one as the time step $\delta t \to 0$.

Taking Remark 2.2 into account, we have

Theorem 3.4. *Let (A1)–(A9) hold. Let $\varphi_0 \in H^3(\Omega)$ satisfies the compatibility condition $\frac{\partial \mu}{\partial \nu} = 0$ a.e. on $\partial\Omega$. Then define the discretization error $e_n = \varphi_n - \varphi^n$, where $\varphi_n = \varphi(n\delta t)$. Assume that the assumptions of Proposition 3.1 and Theorem 3.2 hold. Then, for any $0 < T < \infty$ provided δt is sufficiently small, the sequence e_l with $l \in \mathbb{N}$ such that $l \leqslant \frac{T}{\delta t}$ is bounded in $L^2(\Omega)$, i.e.,*

$$\max_{0 \leqslant l \leqslant T/\delta t} \|e_l\|^2 + \ \delta t \|\nabla e_l\|^2 \leq C(\delta t)^2,$$

where C is a constant which only depends on N, T, Ω, β, σ, J, g, u, and on the initial conditions.

Proof. It follows from (3.1) to (3.3) that

$$\begin{aligned}
&\frac{e_{n+1} - e_n}{\delta t} - c_1 \Delta e_{n+1} - 2\Delta((J_1 \star_\Omega 1)e_{n+1}) + \nabla \cdot (u e_{n+1}) \\
&\quad = \frac{1}{\delta t}(\varphi_{n+1} - \varphi_n) - \frac{1}{\delta t}(\varphi^{n+1} - \varphi^n) - c_1 \Delta \varphi_{n+1} + c_1 \Delta \varphi^{n+1} + \nabla \cdot (u \varphi_{n+1}) \\
&\qquad - \nabla \cdot (u \varphi^{n+1}) - 2\Delta((J_1 \star_\Omega 1)\varphi_{n+1}) + 2\Delta((J_1 \star_\Omega 1)\varphi^{n+1}) \\
&\quad = (\Delta(f(\varphi_n)) - c_1 \Delta \varphi_n - \Delta((J_1 \star_\Omega 1 + J_2 \star_\Omega 1)\varphi_n) - \Delta(J \star_\Omega \varphi_n) - \sigma \varphi_n) + \tau_n \\
&\qquad - (\Delta(f(\varphi^n)) - c_1 \Delta \varphi^n - \Delta((J_1 \star_\Omega 1 + J_2 \star_\Omega 1)\varphi^n) - \Delta(J \star_\Omega \varphi^n) - \sigma \varphi^n) \\
&\quad = -(\Delta(f(\varphi^n) - f(\varphi_n)) - c_1 \Delta(\varphi^n - \varphi_n) - \Delta((J_1 \star_\Omega 1 + J_2 \star_\Omega 1)(\varphi^n - \varphi_n)) \\
&\qquad - \Delta(J \star_\Omega (\varphi^n - \varphi_n)) - \sigma(\varphi^n - \varphi_n)) + \tau_n.
\end{aligned}$$

Therefore, we find

$$\begin{aligned}
e_{n+1} - e_n = {} & c_1 \delta t \Delta(e_{n+1} - e_n) + 2\delta t \Delta((J_1 \star_\Omega 1)e_{n+1}) - \delta t \nabla \cdot (u e_{n+1}) - \delta t \Delta(J \star_\Omega e_n) \\
& + \delta t \Delta(f(\varphi_n) - f(\varphi^n)) - \delta t \Delta((J_1 \star_\Omega 1 + J_2 \star_\Omega 1)e_n) - \sigma \delta t e_n + \delta t \tau_n.
\end{aligned} \tag{3.25}$$

Integrating (3.25) over Ω, we get

$$\frac{1}{\delta t} \langle e_{n+1} - e_n \rangle + \sigma \langle e_n \rangle = \langle \tau_n \rangle . \tag{3.26}$$

Using the fact that $e_0 \equiv 0$, we have

$$\langle e_0 \rangle = 0$$

and, owing to (3.5), we obtain

$$\frac{1}{\delta t} \langle e_1 \rangle = O(\delta t).$$

So by mathematical induction, assuming that the assertion is true for $n = k$, *i.e.*,

$$\frac{1}{\delta t} \langle e_k \rangle = O(\delta t),$$

we find, thanks to (3.26) and (3.5),

$$\frac{1}{\delta t} \langle e_{k+1} - e_k \rangle + \sigma \langle e_k \rangle = \langle \tau_k \rangle .$$

Hence, we have that

$$\frac{1}{\delta t} \langle e_{k+1} \rangle + (\sigma \delta t - 1) O(\delta t) = O(\delta t),$$

which yields

$$\langle e_{k+1}\rangle = O((\delta t)^2)$$

and

$$\langle e_n\rangle = O((\delta t)^2), \quad \forall n \geqslant 1. \tag{3.27}$$

We multiply (3.25) by $2\,e_{n+1}$. This gives

$$\begin{aligned}\|e_{n+1}\|^2 - \|e_n\|^2 + \|e_{n+1}-e_n\|^2 &= -2\delta t(\nabla(f(\varphi_n)-f(\varphi^n)),\nabla e_{n+1})\\ &\quad - 4\delta t(\nabla((J_1\star_\Omega 1)e_{n+1}),\nabla e_{n+1}) - 2c_1\delta t(\nabla(e_{n+1}-e_n),\nabla e_{n+1})\\ &\quad + 2\delta t(ue_{n+1},\nabla e_{n+1}) + 2\delta t(\nabla((J_1\star_\Omega 1 + J_2\star_\Omega 1)e_n),\nabla e_{n+1})\\ &\quad + 2\delta t(\nabla(J\star_\Omega e_n),\nabla e_{n+1}) - 2\sigma\delta t(e_n,e_{n+1}) + 2\delta t(\tau_n,e_{n+1})\\ &= \mathrm{I}+\mathrm{II}+\mathrm{III}+\mathrm{IV}+\mathrm{V}+\mathrm{VI}+\mathrm{VII}+\mathrm{VIII}.\end{aligned} \tag{3.28}$$

Note that, since f' is locally Lipschitz continuous, then

$$\begin{aligned}\mathrm{I} &= 2\delta t(-f'(\varphi^n)\nabla e_n + \nabla\varphi_n(f'(\varphi^n)-f'(\varphi_n)),\nabla e_{n+1})\\ &\leqslant 2\beta\delta t\|\nabla e_n\|\|\nabla e_{n+1}\| + 2c\delta t\|\nabla\varphi_n\|_{L^\infty(\Omega)}\|e_n\|\|\nabla e_{n+1}\|\\ &\leqslant \beta\delta t\|\nabla e_n\|^2 + \frac{c^2\|\nabla\varphi_n\|^2_{L^\infty(\Omega)}}{\kappa}\delta t\|e_n\|^2 + (\beta+\kappa)\delta t\|\nabla e_{n+1}\|^2,\end{aligned} \tag{3.29}$$

for all $\kappa > 0$. Arguing as for the estimates obtained above ((3.10), (3.11) and (3.13)–(3.17)) we find

$$\begin{aligned}\mathrm{II} &\leqslant -4\delta t\int_\Omega (J_1\star_\Omega 1)|\nabla e_{n+1}|^2\mathrm{d}x\\ &\quad + \frac{4}{\kappa}\delta t\|J_1\|^2_{W^{1,1}}\|e_{n+1}\|^2 + \kappa\delta t\|\nabla e_{n+1}\|^2,\end{aligned} \tag{3.30}$$

$$\mathrm{III} \leqslant -c_1\delta t\|\nabla e_{n+1}\|^2 + c_1\delta t\|\nabla e_n\|^2, \tag{3.31}$$

$$\mathrm{IV} \leqslant \kappa\delta t\|\nabla e_{n+1}\|^2 + \frac{\|u\|^2_{L^\infty(\Omega)}}{\kappa}\delta t\|e_{n+1}\|^2, \tag{3.32}$$

$$\begin{aligned}\mathrm{V} &\leqslant \delta t\int_\Omega (J_1\star_\Omega 1 + J_2\star_\Omega 1)|\nabla e_{n+1}|^2\,\mathrm{d}x + \delta t\int_\Omega (J_1\star_\Omega 1 + J_2\star_\Omega 1)|\nabla e_n|^2\,\mathrm{d}x\\ &\quad + \frac{c}{\kappa}\delta t(\|J_1\|^2_{W^{1,1}} + \|J_2\|^2_{W^{1,1}})\|e_n\|^2 + \kappa\delta t\|\nabla e_{n+1}\|^2,\end{aligned} \tag{3.33}$$

$$\mathrm{VI} \leqslant \frac{\|J\|^2_{W^{1,1}}}{\kappa}\delta t\|e_n\|^2 + \kappa\delta t\|\nabla e_{n+1}\|^2, \tag{3.34}$$

$$\mathrm{VII} \leqslant \sigma\delta t\|e_n\|^2 + \sigma\delta t\|e_{n+1}\|^2, \tag{3.35}$$

for all $\kappa > 0$. From Proposition 3.1 and (3.27), we further have

$$\begin{aligned}\mathrm{VIII} &\leqslant 2c\,\delta t\|\tau_n\|_{(H^1(\Omega))^{\star_\Omega}}\|e_{n+1}\|_{H^1(\Omega)}\\ &\leqslant \kappa\delta t\|e_{n+1}\|^2_{H^1(\Omega)} + C(\delta t)^2\delta t\\ &\leqslant \kappa\delta t(\|\nabla e_{n+1}\|^2 + \langle e_{n+1}\rangle^2) + C(\delta t)^2\delta t\\ &\leqslant \kappa\delta t\|\nabla e_{n+1}\|^2 + C(\delta t)^3,\end{aligned} \tag{3.36}$$

where $C > 0$. Combining the above results, we infer

$$\begin{aligned}
\|e_{n+1}\|^2 - \|e_n\|^2 + \delta t \int_\Omega \Big[c_1 + 4(J_1 \star_\Omega 1) - (J_1 \star_\Omega 1 + J_2 \star_\Omega 1) - \beta - 6\kappa\Big] |\nabla e_{n+1}|^2 \, \mathrm{d}x \\
\leqslant \delta t \int_\Omega \Big[c_1 + (J_1 \star_\Omega 1 + J_2 \star_\Omega 1) + \beta\Big] |\nabla e_n|^2 \, \mathrm{d}x \\
+ \delta t \left(\frac{c(\|J_1\|^2_{W^{1,1}} + \|J_2\|^2_{W^{1,1}})}{\kappa} + \frac{\|J\|^2_{W^{1,1}}}{\kappa} + \frac{c^2 \|\nabla \varphi_n\|^2_{L^\infty(\Omega)}}{\kappa} + \sigma \right) \|e_n\|^2 \\
+ \delta t \left(\frac{4\|J_1\|^2_{W^{1,1}}}{\kappa} + \frac{\|u\|^2_{L^\infty(\Omega)}}{\kappa} + \sigma \right) \|e_{n+1}\|^2 + C(\delta t)^3,
\end{aligned}$$

with C independent of δt and l. Summing over n from $n = 0$ to $n = l - 1$ and using the fact that $e_0 \equiv 0$, we obtain

$$\begin{aligned}
\|e_l\|^2 + \delta t \int_\Omega (2\zeta(x) - 6\kappa) \sum_{n=1}^{l-1} |\nabla e_n|^2 \, \mathrm{d}x + \delta t \int_\Omega (\zeta(x) + 2(J_1 \star_\Omega 1) + c_1 - 6\kappa) |\nabla e_l|^2 \mathrm{d}x \\
\leq \left(\frac{c(\|J_1\|^2_{W^{1,1}} + \|J_2\|^2_{W^{1,1}})}{\kappa} + \frac{\|J\|^2_{W^{1,1}}}{\kappa} + \frac{c^2 \|\nabla \varphi_n\|^2_{L^\infty(\Omega)}}{\kappa} + \sigma \right) \delta t \sum_{n=0}^{l-1} \|e_n\|^2 \\
+ \left(\frac{4\|J_1\|^2_{W^{1,1}}}{\kappa} + \frac{\|u\|^2_{L^\infty(\Omega)}}{\kappa} + \sigma \right) \delta t \sum_{n=0}^{l-1} \|e_{n+1}\|^2 + Cl(\delta t)^3, \qquad (3.37)
\end{aligned}$$

where we have used, on account of (3.6), that $\zeta(x) = (J \star_\Omega 1)(x) - \beta > 0$, for almost any x in Ω. Taking $3\kappa < \zeta(x)$, for almost any $x \in \Omega$, we obtain

$$2\zeta(x) - 6\kappa > 0, \quad \text{for} \quad \text{a.a.} \quad x \in \Omega, \qquad (3.38)$$

and

$$\zeta(x) + 2(J_1 \star_\Omega 1) + c_1 - 6\kappa \geqslant 1, \quad \text{for} \quad \text{a.a.} \quad \text{x} \in \Omega. \qquad (3.39)$$

Proceeding as in the proof of Theorem 3.2, we introduce the constants

$$C_1' = \frac{4\|J_1\|^2_{W^{1,1}}}{\kappa} + \frac{\|u\|^2_{L^\infty(\Omega)}}{\kappa} + \sigma$$

and

$$C_2' = \frac{c(\|J_1\|^2_{W^{1,1}} + \|J_2\|^2_{W^{1,1}})}{\kappa} + \frac{\|J\|^2_{W^{1,1}}}{\kappa} + \frac{c^2 \|\nabla \varphi_n\|^2_{L^\infty(\Omega)}}{\kappa} + \sigma$$

and obtain

$$\|e_l\|^2 (1 - \delta t C_1') + \delta t \|\nabla e_l\|^2 \leq \delta t (C_1' + C_2') \sum_{n=1}^{l-1} \|e_n\|^2 + Cl(\delta t)^3.$$

Then, dividing the last inequality by $(1 - \delta t C_1')$ and choosing $\delta t < \frac{1}{2C_1'}$ and $l\delta t \leqslant T$ yields

$$\|e_l\|^2 + \delta t \|\nabla e_l\|^2 \leq 2\delta t (C_1' + C_2') \sum_{n=1}^{l-1} \|e_n\|^2 + 2Cl(\delta t)^3.$$

An application of the discrete Gronwall Lemma entails

$$\|e_l\|^2 + \delta t \|\nabla e_l\|^2 \ \leq C(\delta t)^2,$$

with C independent of δt and l. □

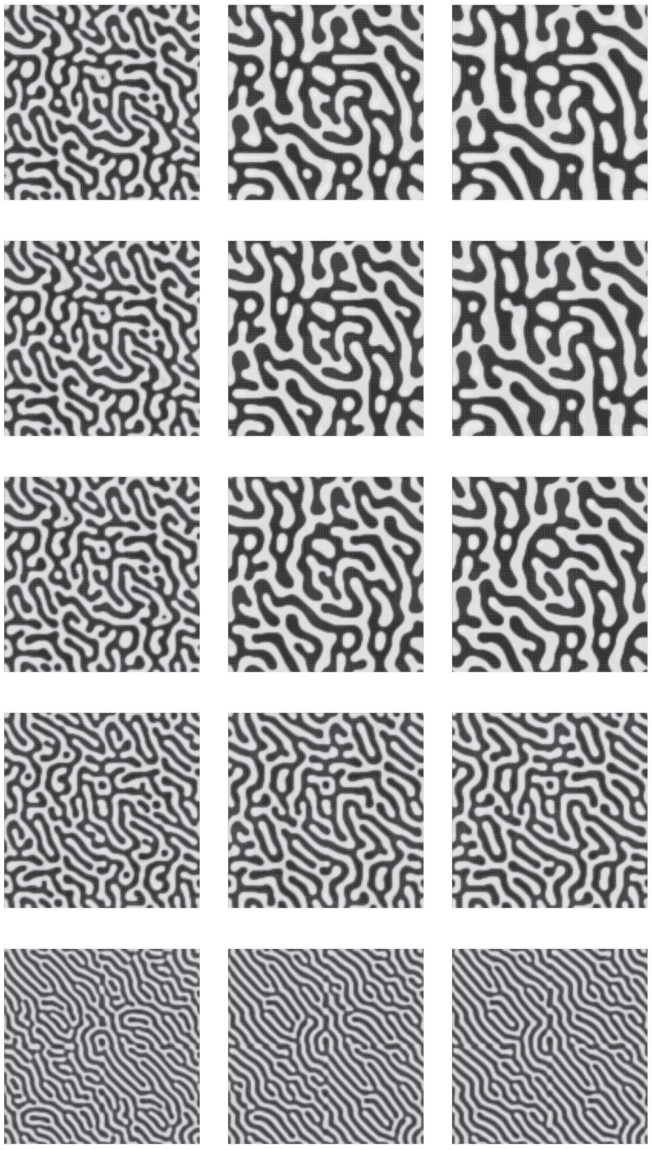

FIGURE 1. $J = J_*$, $u \equiv 0$, $f(s) = s^3 - s$, $m = \langle \varphi_0 \rangle \approx 0$. *First column*: solutions at $T = 0.4$. *Second column*: solutions at $T = 1.2$. *Third column*: solutions at $T = 2$. *First row*: $\sigma = 0$, *second row*: $\sigma = 0.5$, *third row*: $\sigma = 2$, *fourth row*: $\sigma = 10$, *fifth row*: $\sigma = 50$.

4. Numerical simulations

In the time-stepping scheme (3.1) and (3.2), we use a P1-finite element for the space discretization. The numerical simulations are performed with the software Freefem++ (see [33]).

In the numerical results presented below, Ω is a $(-5, 5) \times (-5, 5)$-square, so that we can use the DFFT function to compute the nonlocal terms.

The numerical simulations presented below show the efficiency of the model not only for phase separation phenomena, but also for crystal nucleation. In particular, when $\sigma = 0$, and $u \equiv g \equiv 0$, the results can be

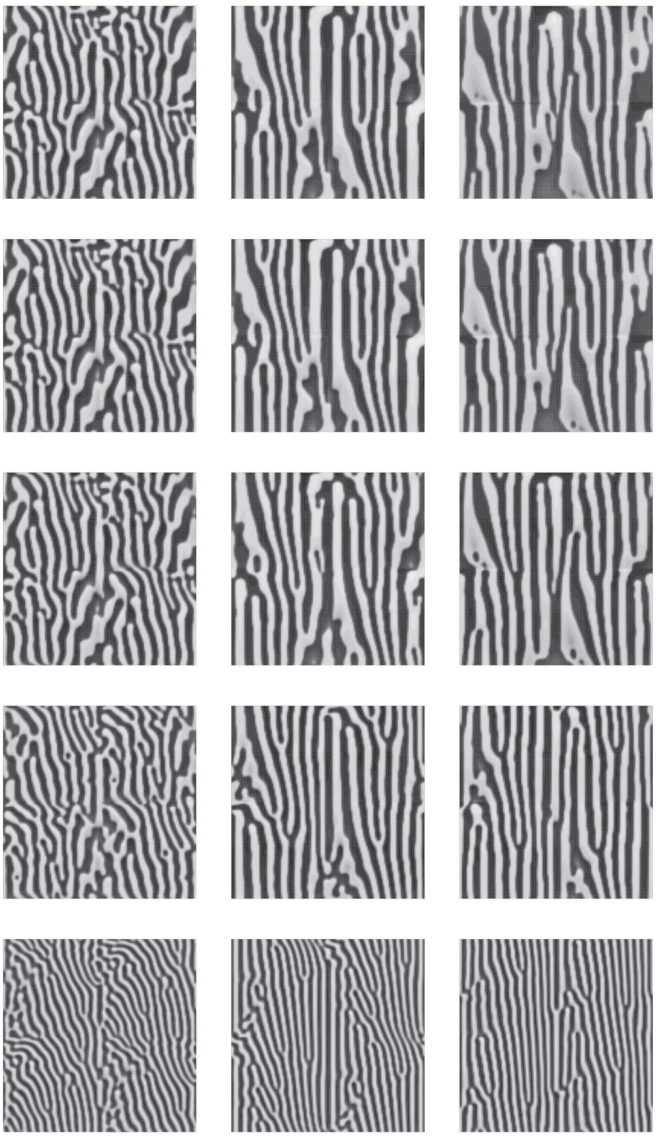

FIGURE 2. $J = J_*$, $u = (0, xy(10-x)(10-y)/20)$, $f(s) = s^3 - s$, $m = \langle \varphi_0 \rangle \approx 0$. *First column*: solutions at $T = 0.4$. *Second column*: solutions at $T = 1.2$. *Third column*: solutions at $T = 2$. *First row*: $\sigma = 0$, *second row*: $\sigma = 0.5$, *third row*: $\sigma = 2$, *fourth row*: $\sigma = 10$, *fifth row*: $\sigma = 50$.

compared with the ones presented in [29, 30]. The simulations presented below illustrate, from the numerical point of view, the modified nonlocal model proposed by Bates and Han with varying values of σ, with varying values of m (which characterizes of the loss of mass in the model) and varying values of u (corresponding to a transport term that accounts for a possible flow of the mixture at a certain given velocity field u). In each picture, the maximum value of $\varphi \approx 1$ is colored in black , the minimum value of $\varphi \approx -1$ in white, and the values of φ in between correspond to different shades of grey.

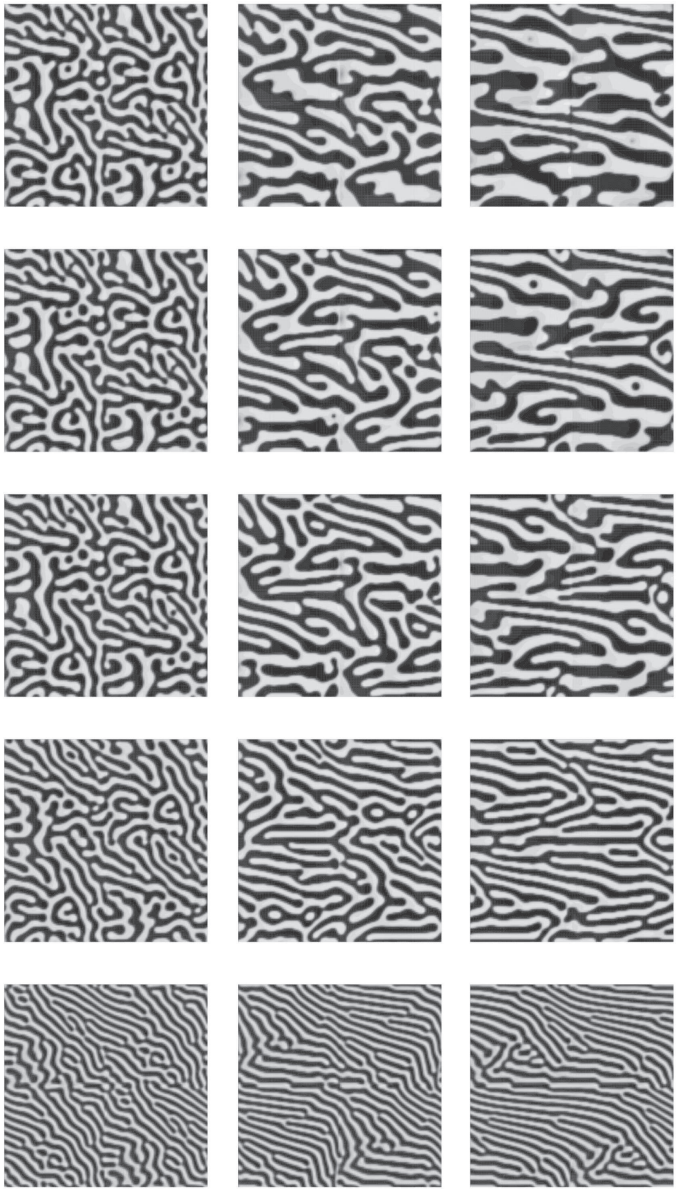

FIGURE 3. $J = J_*$, $u = (xy(10-x)(10-y)/50, 0)$, $f(s) = s^3 - s$, $m = \langle \varphi_0 \rangle \approx 0$. *First column*: solutions at $T = 0.4$. *Second column*: solutions at $T = 1.2$. *Third column*: solutions at $T = 2$. *First row*: $\sigma = 0$, *second row*: $\sigma = 0.5$, *third row*: $\sigma = 2$, *fourth row*: $\sigma = 10$, *fifth row*: $\sigma = 50$.

4.1. Phase separation and coarsening: dynamics of the solutions of the nonlocal Cahn–Hilliard–Oono equation with positive Gaussian kernel

Here, the triangulation of Ω is obtained by dividing Ω into 128×128 rectangles and by dividing each rectangle along the same diagonal.

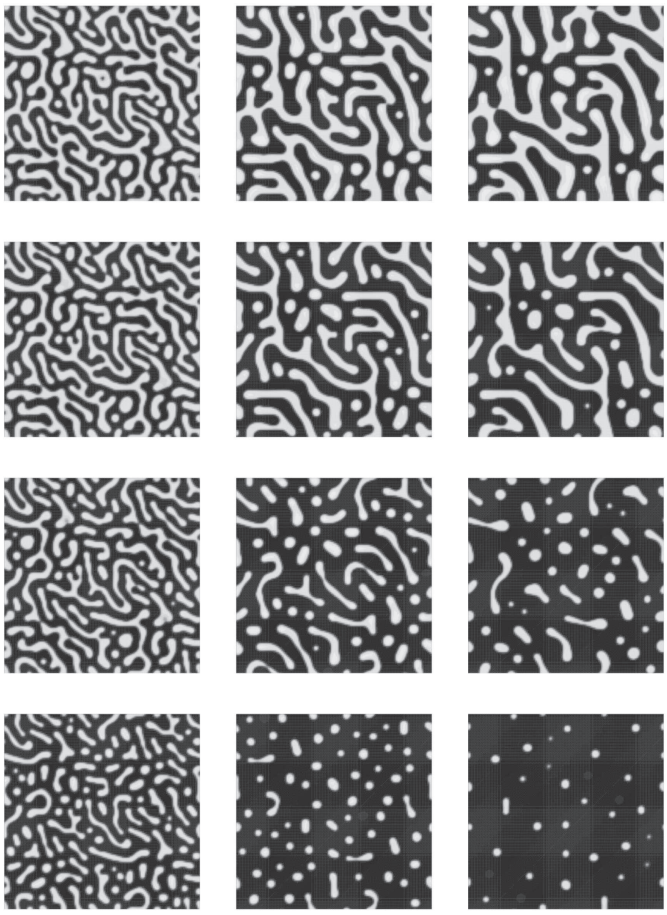

FIGURE 4. $J = J_*$, $u \equiv 0$, $f(s) = s^3 - s$, $\langle \varphi_0 \rangle \approx 0$, $m = 1$. *First column*: solutions at $T = 0.4$. *Second column*: solutions at $T = 1.2$. *Third column*: solutions at $T = 2$. *First row*: $\sigma = 0.05$, *second row*: $\sigma = 0.2$, *third row*: $\sigma = 0.5$, and *fourth row*: $\sigma = 1$.

Dynamics of the solutions with a null transport term

In Figure 1, we consider a random initial datum between -0.05 and 0.05, which leads to a spatial average close to 0. In that case, the interaction kernel $J := J_*$ is given by a positive Gaussian function defined as follows

$$J_*(x_1, x_2) = \frac{1}{\varepsilon_1^2}\, e^{-\frac{{x_1}^2 + {x_2}^2}{\varepsilon_1^2}} \tag{4.1}$$

where $\varepsilon_1 = 0.05$. Furthermore, we consider the typical choice of the nonlinear term $f(s) = s^3 - s$ and take $m = \langle \varphi_0 \rangle \approx 0$. The parameters of the numerical simulations are $h = \frac{10}{128}$, $\delta t = 2 \times 10^{-4}$, $u \equiv (0, 0)$, and $g = 0$. The final time for the simulation is $T = 2$.

For $\sigma = 0$, we present the dynamics of the solution to the nonlocal Cahn–Hilliard equation at $T = 0.4$, $T = 1.2$, and $T = 2$, respectively.

Note that, when σ is close to zero, the dynamics of the nonlocal Cahn–Hilliard–Oono equation is close to that of the nonlocal Cahn–Hilliard equation. Finally, we show the effects of the long-range interactions on the

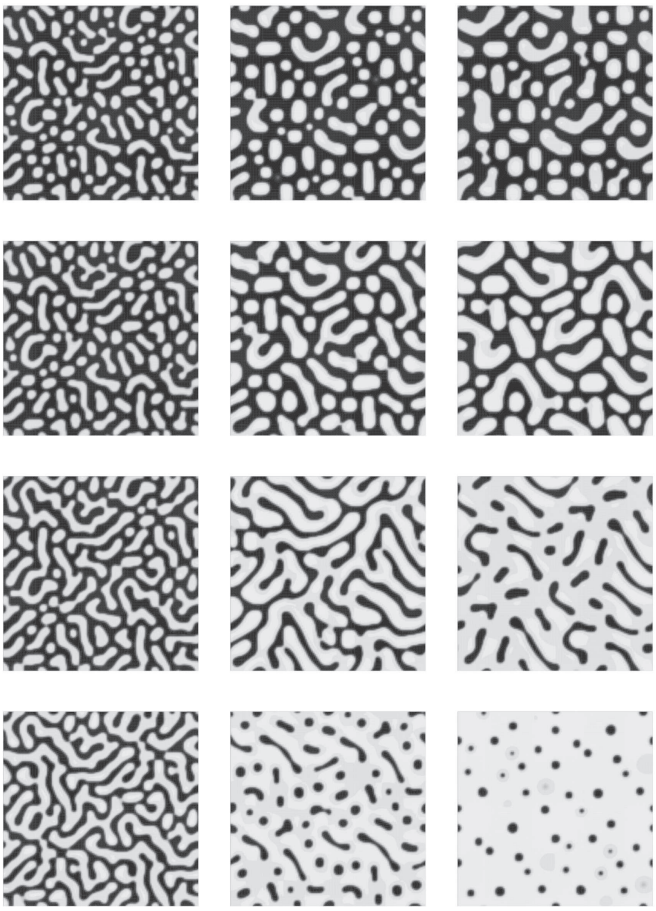

FIGURE 5. $J = J_*$, $u \equiv 0$, $f(s) = s^3 - s$, $\langle \varphi_0 \rangle \approx 0.2$, $m = -1$. *First column*: solutions at $T = 0.4$. *Second column*: solutions at $T = 1.2$. *Third column*: solutions at $T = 2$. *First row*: $\sigma = 0.05$, *second row*: $\sigma = 0.2$, *third row*: $\sigma = 0.5$, and *fourth row*: $\sigma = 1$.

nonlocal Cahn–Hilliard equation with $\sigma = 0.5$, $\sigma = 2$, $\sigma = 10$ and $\sigma = 50$ respectively. As it was noticed in [2], we observe that the coarsening is inhibited for large values of σ.

Effects of the transport term

We present in Figures 2 and 3 the evolution of the nonlocal Cahn–Hilliard–Oono equation again, with the same parameters and functions as in Figure 1, but we now take a non-vanishing transport term. First, in Figure 2, we take a transport term $u = (0,\, xy(10-x)(10-y)/20)$ and then, in Figure 3, we take $u = (xy(10-x)(10-y)/50,\, 0)$. In both cases, the influence of the velocity field on the pattern formation phenomenon is clearly visible. In particular, the choice of a vertical transport term in Figure 2 shows that the corresponding evolution is distinctly vertical for different choices of σ and similarly, the choice of an horizontal transport term in Figure 3 shows that the corresponding evolution is distinctly horizontal for different choices of σ.

Off critical case (*i.e.*, $m \neq \langle \varphi_0 \rangle$)

We present in Figures 4 and 5 the evolution of the nonlocal Cahn–Hilliard–Oono equation, with the same parameters and functions as in Figure 1, but we now assume loss of mass (*i.e.*, $m \neq \langle \varphi_0 \rangle$), where $\langle \varphi_0 \rangle \approx 0$ and

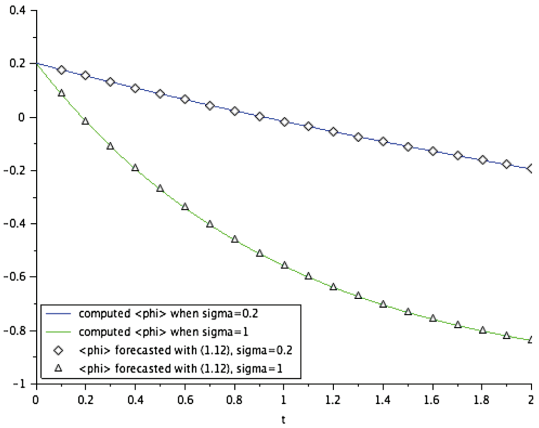

FIGURE 6. Computed and predicted values of $\langle\varphi\rangle$ with respect to time, when $\sigma = 0.2$ and $\sigma = 1$ (*cf.* Fig. 5).

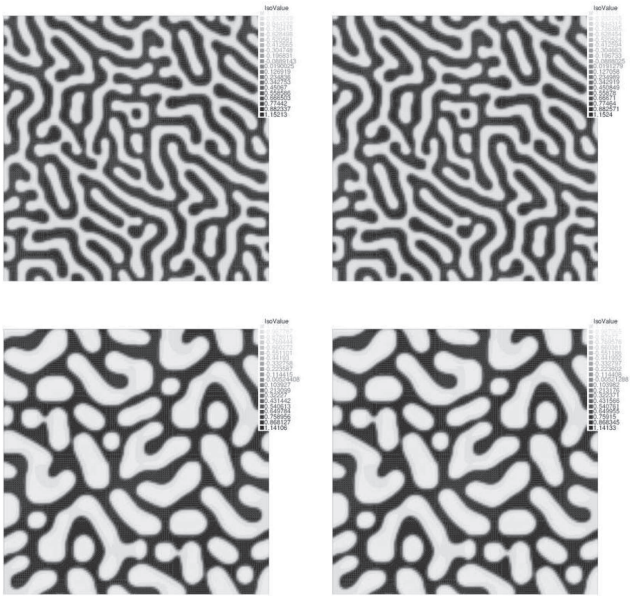

FIGURE 7. *First line*: solutions at $t = 2$, under the conditions of Figure 1, $\sigma = 10$, with the potential $f(s) = s^3 - s$ (*left*) and with the quadratic regularized potential defined by (2.1) (*right*). *Second line*: solutions at $t = 2$, under the conditions of Figure 5, $\sigma = 0.2$, with the potential $f(s) = s^3 - s$ (*left*) and with the quadratic regularized potential defined by (2.1) (*right*).

$m = 1$ in Figure 4 and $\langle\varphi_0\rangle \approx 0.2$ (φ_0 randomly distributed between -0.3 and 0.7) and $m = -1$ in Figure 5. We emphasize that our results are consistent with (1.14). Indeed, when $m = \langle\varphi_0\rangle$, the quantity $\langle\varphi\rangle$ is conserved. Moreover, when $m \neq \langle\varphi_0\rangle$ the spatial average follows perfectly the predicted values given by (1.14) (see Fig. 6).

In Figure 7, we compare the solutions, under the conditions of Figures 1 and 5, obtained with the "physical" potential $f(s) = s^3 - s$ and with the quadratic regularized potential arising from (2.1). As it can be noticed,

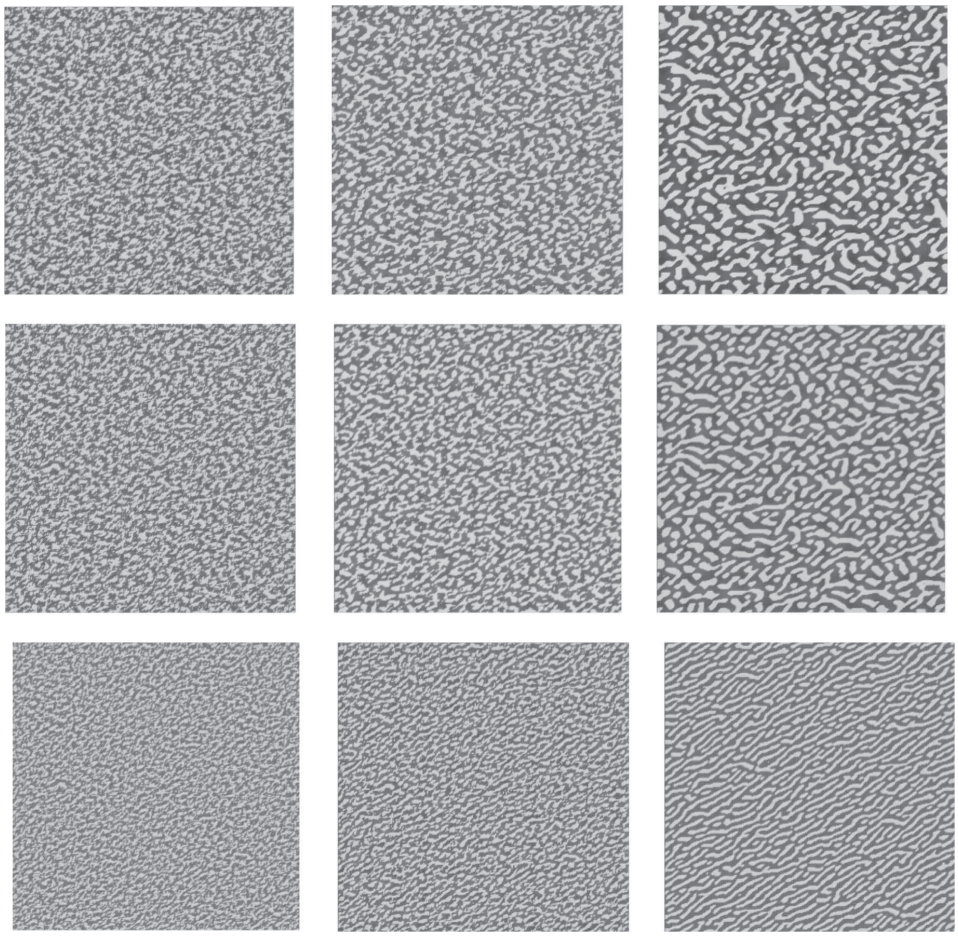

FIGURE 8. $J = J_a$, $u \equiv 0$, $f(s) = s^3 - s$, $m = \langle \varphi_0 \rangle \approx 0.2$. *First column*: solutions at $T = 0.5$. *Second column*: solutions at $T = 1$. *Third column*: solutions at $T = 5$. *First row*: $\sigma = 0$, *second row*: $\sigma = 5$ and *third row*: $\sigma = 50$.

with both potentials, the computed solutions stay in the interval $[-1.15; 1, 15]$, leading to quite similar solutions and justifying our modified potential.

4.2. Nucleation and growth with an anisotropic kernel

Here, the triangulation of Ω is obtained by dividing Ω into 300×300 rectangles and by dividing each rectangle along the same diagonal.

Six-fold anisotropic shape (*cf.* [30] for this terminology)

In Figure 8, we consider a random initial datum between -0.3 and 0.7, which leads to a spatial average close to 0.2. In that case, the interaction kernel J_a (in view of [30] where the nucleation and growth in this case are very similar to the simulations of the anisotropic PFC equation) is given by the difference of two positive

Gaussian functions defined as

$$
\begin{aligned}
J_a(x_1,x_2) = {} & \frac{0.1}{3\varepsilon_1^2}\, e^{\left(-\frac{x_1^2}{\varepsilon_1^2}-\frac{4x_2^2}{\varepsilon_1^2}\right)} + \frac{0.1}{3\varepsilon_1^2}\, e^{\left(-\frac{\left(\frac{x_1}{2}-\frac{\sqrt{3}x_2}{2}\right)^2}{\varepsilon_1^2}-\frac{4\left(\frac{\sqrt{3}x_1}{2}+\frac{x_2}{2}\right)^2}{\varepsilon_1^2}\right)} \\
& + \frac{0.1}{3\varepsilon_1^2}\, e^{\left(-\frac{\left(\frac{x_1}{2}-\frac{\sqrt{3}x_2}{2}\right)^2}{\varepsilon_1^2}-\frac{4\left(\frac{\sqrt{3}x_1}{2}-\frac{x_2}{2}\right)^2}{\varepsilon_1^2}\right)} - \frac{0.08}{3\varepsilon_2^2}\, e^{\left(-\frac{x_1^2}{\varepsilon_2^2}-\frac{4x_2^2}{\varepsilon_2^2}\right)} \\
& - \frac{0.08}{3\varepsilon_2^2}\, e^{\left(-\frac{\left(\frac{x_1}{2}-\frac{\sqrt{3}x_2}{2}\right)^2}{\varepsilon_2^2}-\frac{4\left(\frac{\sqrt{3}x_1}{2}+\frac{(x_2)}{2}\right)^2}{\varepsilon_2^2}\right)} - \frac{0.08}{3\varepsilon_2^2}\, e^{\left(-\frac{(\frac{x_1}{2}-\frac{\sqrt{3}x_2}{2})^2}{\varepsilon_2^2}-\frac{4\left(\frac{\sqrt{3}x_1}{2}-\frac{x_2}{2}\right)^2}{\varepsilon_2^2}\right)}
\end{aligned}
\tag{4.2}
$$

where $\varepsilon_1 = 0.08$, $\varepsilon_2 = 0.2$. Furthermore, we take $f(s) = s^3 - s$. The parameters of the numerical simulations are $h = \frac{10}{300}$, $\delta t = 10^{-2}$, $m = \langle \varphi_0 \rangle$, $u = (0,0)$, and $g = 0$. The final time for the simulations is $T = 5$. We present the results for the nonlocal Cahn–Hilliard equation ($\sigma = 0$) and the nonlocal Cahn–Hilliard–Oono equation for $\sigma = 0.05$ at $T = 0.5$, $T = 1$, and $T = 5$.

Acknowledgements. The authors wish to thank the referees for their careful reading of the article as well as for their useful comments. The third author thanks the Laboratoire de Mathématiques et Applications de L'Université de Poitiers for its kind hospitality which allowed all the authors to exchange their ideas on this research subject. The third author is a member of the Gruppo Nazionale per l'Analisi Matematica, la Probabilità e le loro applicazioni (GNAMPA) of the Istituto Nazionale di Alta Matematica (INdAM).

References

[1] N. Abukhdeir, D. Vlachos, M. Katsoulakis and M. Plexousakis, Long-time integration methods for mesoscopic models of pattern-forming systems. *J. Comput. Phys.* **18** (2013) 2211–2238.

[2] A.C. Aristotelous, O. Karakashian and S.M. Wise, A mixed discontinuous Galerkin, convex splitting scheme for a modified Cahn–Hilliard equation and an efficient nonliniear multigrid solver. *Disc. Cont. Dyn. Syst. B* **20** (2015) 1529–1553.

[3] P.W. Bates and J. Han, The Neumann boundary problem for a nonlocal Cahn–Hilliard equation. *J. Diff. Equ.* **212** (2005) 235–277.

[4] P.W. Bates and J. Han, The Dirichlet boundary problem for a nonlocal Cahn–Hilliard equation. *J. Math. Anal. App.* **311** (2005) 289–312.

[5] P.W. Bates, S. Brown and J. Han, Numerical analysis for a nonlocal Allen–Cahn equation. *Int. J. Numer. Anal. Model.* **6** (2009) 33–49.

[6] A. Bertozzi, S. Esedoglu and A. Gillette, Analysis of a two-scale Cahn–Hilliard model for binary image inpainting. *Multiscale Model. Simul.* **6** (2007) 913–936.

[7] L.A. Caffarelli and N.E. Muler, An L^∞ bound for solutions of the Cahn–Hilliard equation. *Arch. Ration. Mech. Anal.* **135** (1995) 129–144.

[8] J.W. Cahn and J.E. Hilliard, Free energy of a nonuniform system I. Interfacial free energy. *J. Chem. Phys.* **28** (1958) 258–267.

[9] L. Cherfils, A. Miranville and S. Zelik, The Cahn–Hilliard equation with logarithmic potentials. *Milan J. Math.* **79** (2011) 561–596.

[10] L. Cherfils, A. Miranville and S. Zelik, On a generalized Cahn–Hilliard equation with biological applications. *Disc. Cont. Dyn. Sys. B* **19** (2014) 2013–2026.

[11] L. Cherfils, H. Fakih and A. Miranville, Finite-dimensional attractors for the Bertozzi–Esedoglu–Gillette–Cahn–Hilliard equation in image inpainting. *Inv. Prob. Imag.* **9** (2015) 105–125.

[12] L. Cherfils, H. Fakih and A. Miranville, On the Bertozzi–Esedoglu–Gillette–Cahn–Hilliard equation with logarithmic nonlinear terms. *SIAM J. Imag. Sci.* **8** (2015) 1123–1140.

[13] L. Cherfils, H. Fakih and A. Miranville, A Cahn–Hilliard system with a fidelity term for color image inpainting. *J. Math. Imag. Vision* **54** (2016) 117–131.

[14] L. Cherfils, H. Fakih and A. Miranville, A complex version of the Cahn–Hilliard equation for grayscale image inpainting. *Multiscale Model. Simul.* **15** (2017) 575–605.

[15] D. Cohen and J.M. Murray, A generalized diffusion model for growth and dispersion in a population. *J. Math. Biol.* **12** (1981) 237–248.

[16] E. Davoli, L. Scarpa and L. Trussardi, Local asymptotics for nonlocal convective Cahn–Hilliard equations with $W^{1,1}$ kernel and singular potential. Preprint arXiv:1911.12770v1 [math.AP] (2019).

[17] E. Davoli, H. Ranetbauer, L. Scarpa and L. Trussardi, Degenerate nonlocal Cahn–Hilliard equations: well-posedness, regularity and local asymptotics. *Ann. Inst. Henri Poincaré C, Anal. non Lin.* **37** (2020) 627–651.

[18] F. Della Porta and M. Grasselli, Convective nonlocal Cahn–Hilliard equations with reaction terms. *Disc. Cont. Dyn. Syst. B* **20** (2015) 1529–1553.

[19] I.C. Dolcetta, S.F. Vita and R. March, Area-preserving curve-shortening flows: from phase separation to image processing. *Interfaces Free Bound.* **4** (2002) 325–343.

[20] Q. Du, M. Gunzburger, R. LeHoucq and K. Zhou, Analysis and approximation of nonlocal diffusion problems with volume constraints. *SIAM Rev.* **54** (2012) 667–696.

[21] D.J. Eyre, An unconditionally stable one-step scheme for gradient systems. Available at: https://www.math.utah.edu/~eyre/research/methods/stable.ps (2020).

[22] H. Fakih, A Cahn–Hilliard equation with a proliferation term for biological and chemical applications. *Asympt. Anal.* **94** (2015) 71–104.

[23] P.C. Fife, Models for phase separation and their mathematics. *Electron. J. Diff. Equ.* **13** (2002) 353–370.

[24] H. Gajewski and K. Gärtner, On a nonlocal model of image segmentation. *Z. Angew. Math. Phys.* **56** (2005) 572–591.

[25] C.G. Gal, A. Giorgini and M. Grasselli, The nonlocal Cahn–Hilliard equation with singular potential: well-posedness, regularity and strict separation property. *J. Differ. Equ.* **263** (2017) 5253–5297.

[26] G. Giacomin and J.L. Lebowitz, Exact macroscopic description of phase segregation in model alloys with long range interactions. *Phys. Rev. Lett.* **76** (1996) 1094–1097.

[27] A. Giorgini, M. Grasselli and A. Miranville, The Cahn–Hilliard–Oono equation with singular potential. *Math. Models Methods Appl. Sci.* **27** (2017) 2485–2510.

[28] M. Grasselli and H. Wu, Well-posedness and longtime behavior for the modified phase-field crystal equation. *Math. Models Methods Appl. Sci.* **24** (2014) 2743–2783.

[29] Z. Guan, C. Wang and S.M. Wise, A Convergent convex splitting scheme for the periodic nonlocal Cahn–Hilliard equation. *Numer. Math.* **128** (2014) 377–406.

[30] Z. Guan, J.S. Lowengrub, C. Wang and S.M. Wise, Second-order convex splitting schemes for periodic nonlocal Cahn–Hilliard and Allen–Cahn equations. *J. Comput. Phys.* **277** (2014) 48–71.

[31] Z. Guan, J.S. Lowengrub and C. Wang, Convergence analysis for second order accurate convex splitting schemes for the periodic nonlocal Allen–Cahn and Cahn–Hilliard equations. *Math. Methods Appl. Sci.* **40** (2017) 6836–6863.

[32] T. Hartley and T. Wanner, A semi-implicit spectral method for stochastic nonlocal phase-field models. *Disc. Cont. Dyn. Syst.* **25** (2009) 399–429.

[33] F. Hecht, New development in FreeFem++. *J. Numer. Math.* **20** (2012) 251–265.

[34] D. Hornthrop, M. Katsoulakis and D. Vlachos, Spectral methods for mesoscopic models of pattern formation. *J. Comput. Phys.* **173** (2001) 364–390.

[35] E. Khain and L.M. Sander, A generalized Cahn–Hilliard equation for biological applications. *Phys. Rev. E* **77** (2008) 051129.

[36] I. Klapper and J. Dockery, Role of cohesion in the material description of biofilms. *Phys. Rev. E* **74** (2006) 0319021.

[37] J.S. Langer, Theory of spinodal decomposition in alloys. *Ann. Phys.* **65** (1975) 53–86.

[38] Q.-X. Liu, A. Doelman, V. Rottschäfer, M. de Jager, P.M.J. Herman, M. Rietkerk and J. van de Koppel, Phase separation explains a new class of self-organized spatial patterns in ecological systems. *Proc. Nat. Acad. Sci.* **110** (2013), 11905–11910.

[39] S. Maier-Paape and T. Wanner, Spinodal decomposition for the Cahn–Hilliard equation in higher dimensions: nonlinear dynamics. *Arch. Ration. Mech. Anal.* **151** (2000) 187–219.

[40] S. Melchionna and E. Rocca, On a nonlocal Cahn–Hilliard equation with a reaction term. *Adv. Math. Sci. App.* **24** (2014) 461–497.

[41] A. Miranville, Asymptotic behavior of the Cahn–Hilliard–Oono equation. *J. Appl. Anal. Comput.* **1** (2011) 523–536.

[42] A. Miranville and S. Zelik, The Cahn–Hilliard equation with singular potentials and dynamic boundary conditions. *Disc. Cont. Dyn. Syst.* **28** (2010) 275–310.

[43] C.B. Muratov, Droplet phases in non-local Ginzburg–Landau models with Coulomb repulsion in two dimensions. *Commun. Math. Phys.* **299** (2010) 45–87.

[44] R.H. Nochetto, A.J. Salgado and S.W. Walker, A diffuse interface model for electrowetting with moving contact lines. *Math. Models Methods Appl. Sci.* **24** (2014) 67–111.

[45] Y. Oono and S. Puri, Computationally efficient modeling of ordering of quenched phases. *Phys. Rev. Lett.* **58** (1987) 836–839.

[46] A. Oron, S.H. Davis and S.G. Bankoff, Long-scale evolution of thin liquid films. *Rev. Mod. Phys.* **69** (1997) 931–980.

[47] E.W. Sachs and A.K. Strauss, Efficient solution of a partial integro-differential equation in finance. *Appl. Numer. Math.* **58** (2008) 1687–1703.

[48] C.-B. Schönlieb and A. Bertozzi, Unconditionally stable schemes for higher order inpainting. *Commun. Math. Sci.* **9** (2011) 413–457.

[49] U. Thiele and E. Knobloch, Thin liquid films on a slightly inclined heated plate. *Phys. D* **190** (2004) 213–248.

[50] S. Tremaine, On the origin of irregular structure in Saturn's rings. *Astron. J.* **125** (2003) 894–901.

[51] S. Villain-Guillot, *Phases modulées et dynamique de Cahn–Hilliard*, Habilitation thesis. Université Bordeaux I (2010).

[52] K. Zhou and Q. Du, Mathematical and numerical analysis of linear peridynamic models with nonlocal boundary conditions. *SIAM J. Numer. Anal.* **48** (2010) 1759–1780.